



Federal University of São Carlos

Graduate Program in Chemical Engineering

Master Thesis

**Automation of a reactor for enzymatic
hydrolysis of sugar cane bagasse:
Computational intelligence-based adaptive
control**

Vitor Badiale Furlong

Advisor: Prof. Roberto de Campos Giordano

Coadvisor: Prof. Marcelo Perencin de Arruda Ribeiro

São Carlos - SP

March 20th, 2015

Vitor Badiale Furlong

Automation of a reactor for enzymatic hydrolysis of sugar cane bagasse: Computational intelligence-based adaptive control

Master thesis submitted to the Graduate Program in Chemical Engineering, Center of Exact Sciences and Technology, Federal University of São Carlos, as partial fulfillment of the requirements for degree of Master of Science.

Advisor: Prof. Roberto de Campos Giordano

Coadvisor: Prof. Marcelo Perencin de Arruda Ribeiro

São Carlos - SP

March 20TH, 2015

Ficha catalográfica elaborada pelo DePT da Biblioteca Comunitária UFSCar
Processamento Técnico
com os dados fornecidos pelo(a) autor(a)

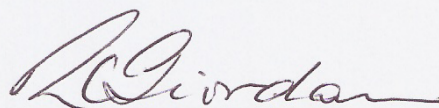
F985a Furlong, Vitor Badiale
Automation of a reactor for enzymatic hydrolysis
of sugar cane bagasse : Computational intelligence-
based adaptive control / Vitor Badiale Furlong. --
São Carlos : UFSCar, 2016.
65 p.

Dissertação (Mestrado) -- Universidade Federal de
São Carlos, 2015.

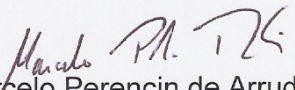
1. Controle ótimo. 2. Monitoramento de hidrólise
enzimática de bagaço de cana-de-açúcar. 3. Perfil de
alimentação ótimos para reator semicontínuo. I. Título.

MEMBROS DA BANCA EXAMINADORA DA DEFESA DE DISSERTAÇÃO DE VITOR BADIALE FURLONG APRESENTADA AO PROGRAMA DE PÓS-GRADUAÇÃO EM ENGENHARIA QUÍMICA DA UNIVERSIDADE FEDERAL DE SÃO CARLOS, EM 20 DE MARÇO DE 2015.

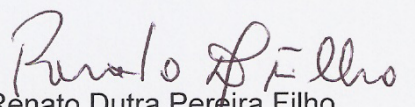
BANCA EXAMINADORA:



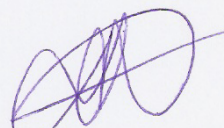
Roberto de Campos Giordano
Orientador, UFSCar



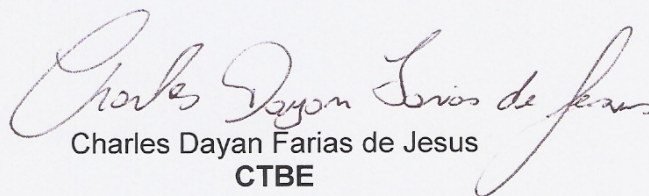
Marcelo Perencin de Arruda Ribeiro
Coorientador, UFSCar



Renato Dutra Pereira Filho
FURG



Daniel Ibraim Pires Atala
BP BIOFUELS



Charles Dayan Farias de Jesus
CTBE

*To my parents.
In retribution to all the love and care.
The feeling is mutual.*

AGRADECIMENTO – ANP

Este trabalho foi desenvolvido no Laboratório de Desenvolvimento e Automação de Bioprocessos do Departamento de Engenharia Química (DEQ) da Universidade Federal de São Carlos (UFSCar) e contou com o apoio financeiro do Programa de Recursos Humanos da Agência Nacional do Petróleo, Gás natural e Biocombustíveis (PRH-ANP/MCT Nº 44).



Agradecimentos Pessoais

Aos Professores Roberto e Marcelo pela dedicação.

A banca examinadora, pela disponibilidade.

A minha família, pelo amor e paciência.

A Fabiane Cristina, pelo amor e por aguentar a minha falta de paciência.

Aos colegas de laboratório, atuais e antigos, amigos e todos aqueles que tem que aguentar o meu mau humor diariamente.

Ao povo brasileiro pelo estudo a mim disponibilizado.

*There are two types of people in the world:
-Those who can extrapolate from incomplete data.*

-

ABSTRACT

The continuous demand growth for liquid fuels, alongside with the decrease of fossil oil reserves, unavoidable in the long term, induces investigations for new energy sources. A possible alternative is the use of bioethanol, produced by renewable resources such as sugarcane bagasse. Two thirds of the cultivated sugarcane biomass are sugarcane bagasse and leaves, not fermentable when the current, first-generation (1G) process is used. A great interest has been given to techniques capable of utilizing the carbohydrates from this material. Among them, production of second generation (2G) ethanol is a possible alternative. 2G ethanol requires two additional operations: a pretreatment and a hydrolysis stage. Regarding the hydrolysis, the dominant technical solution has been based on the use of enzymatic complexes to hydrolyze the lignocellulosic substrate. To ensure the feasibility of the process, a high final concentration of glucose after the enzymatic hydrolysis is desirable. To achieve this objective, a high solid consistency in the reactor is necessary. However, a high load of solids generates a series of operational difficulties within the reactor. This is a crucial bottleneck of the 2G process. A possible solution is using a fed-batch process, with feeding profiles of enzymes and substrate that enhance the process yield and productivity. The main objective of this work was to implement and test a system to infer online concentrations of fermentable carbohydrates in the reactive system, and to optimize the feeding strategy of substrate and/or enzymatic complex, according to a model-based control strategy. Batch and fed-batch experiments were conducted in order to test the adherence of four simplified kinetic models. The model with best adherence to the experimental data (a modified Michaelis-Mentem model with inhibition by the product) was used to train an Artificial Neural Network (ANN) as a softsensor to predict glucose concentrations. Further, this ANN may be used in a closed-loop control strategy. A feeding profile optimizer was implemented, based on the optimal control approach. The ANN was capable of inferring the product concentration from the available data with good adherence (Determination Coefficient of 0.972). The optimization algorithm generated profiles that increased a process performance index while maintaining operational levels within the reactor, reaching glucose concentrations close to those utilized in current first generation technology a (ranging between 156.0 g.L^{-1} and 168.3 g.L^{-1}). However rough estimates for scaling up the reactor to industrial dimensions indicate that this conventional reactor design must be replaced by a two-stage reactor, to minimize the volume of liquid to be stirred.

Key-words: Bagasse Enzymatic Hydrolysis monitoring, Neural Network Inference, Optimal Control, Optimal Feeding Policies for Semi-Continuous Reactor.

RESUMO

A crescente demanda por combustíveis líquidos, bem como a diminuição das reservas de petróleo, inevitáveis a longo prazo, induzem pesquisas por novas fontes de energia. Uma possível solução é o uso do bioetanol, produzido de resíduos, como o bagaço de cana-de-açúcar. Dois terços da biomassa cultivada são bagaço e folhas. Estas frações não são fermentescíveis quando se usa a tecnologia de primeira geração atual (1G). Um grande interesse vem sendo prestado a técnicas capazes de utilizar os carboidratos deste material. Dentre elas, a produção de etanol de segunda geração (2G) é uma possível alternativa. Etanol 2G requer duas operações adicionais: etapas de pré-tratamento e hidrólise. Considerando a hidrólise, a técnica dominante tem sido a utilização de complexos enzimáticos para hidrolisar o substrato lignocelulósico. Para assegurar a viabilidade do processo, uma alta concentração final de glicose é necessária ao final do processo. Para atingir esse objetivo, uma alta concentração de sólidos no reator é necessária. No entanto, uma carga grande de sólidos gera uma série de dificuldades operacionais para o processo. Este é um gargalo crucial do processo 2G. Uma possível solução é utilizar um processo de batelada alimentada, com perfis de alimentação de enzima e substrato para aumentar produtividade e rendimento. O principal objetivo deste trabalho é implementar e testar um sistema para inferir concentração de carboidratos fermentescíveis automaticamente e otimizar a política de substrato e/ou enzima em tempo real, de acordo com uma estratégia de controle baseada em modelo cinético. Experimentos de batelada e batelada alimentada foram realizados a fim de testar a aderência de 4 modelos cinéticos simplificados. O modelo com melhor aderência aos dados experimentais (um modelo de Michaelis-Menten modificado com inibição por produto) foi utilizado para gerar dados a fim de treinar uma rede neural artificial para prever concentrações de glicose automaticamente. Em estudos futuros, esta rede pode ser utilizada para compor o fechamento da malha de controle. Um otimizador de perfil de alimentação foi implementado, este foi baseado em uma abordagem de controle ótimo. A rede neural foi capaz de prever a concentração de produto com os dados disponíveis de maneira satisfatória (Coeficiente de Determinação de 0.972). O algoritmo de otimização gerou perfis que aumentaram a performance do processo enquanto manteve as condições da hidrólise dentro de níveis operacionais, e gerou concentrações de glicose próximas as obtidas pelo caldo de cana-de-açúcar da primeira geração (valores entre 156.0 g.L^{-1} e 168.3 g.L^{-1}). No entanto, estimativas iniciais de aumento de escala do processo demonstraram que para atingir dimensões industriais o projeto do reator utilizado deve ser analisado, substituindo o mesmo por um processo em dois estágios para diminuir o volume do reator e energia para agitação.

Palavras Chave: Controle Ótimo, Monitoramento de Hidrólise Enzimática de Bagaço de Cana-de-açúcar, Perfil de Alimentação Ótimos para Reator Semicontínuo.

FIGURES INDEX

Figure 1 - Lignocellulosic Biomass Processing.....	4
Figure 2 - Monitoring and control system.....	20
Figure 3 - Sensor array coupling.....	21
Figure 4 - Interpolation Example.....	25
Figure 5 - Model Fitting Flowchart.....	29
Figure 6 - Feeding profile optimization.....	31
Figure 7 - Cross Validation Procedure.....	33
Figure 8 - Evaluated transfer functions.....	34
Figure 9 - Training and Validation Data set Error.....	34
Figure 10 - Conductance and glucose concentration during hydrolysis.....	35
Figure 11 - Full Array Monitoring During Batch Experiments.....	36
Figure 12 - Full Array Monitoring During Fed-batch Experiments.....	36
Figure 13 - Supernatant Scans During Fed-batch Experiments.....	37
Figure 14 - Supernatant Scans from 250 to 320 nm.....	37
Figure 15 - Experimental Data for Batch Experiments.....	38
Figure 16 - Experimental Data for Fed-batch Experiments.....	39
Figure 17 - Batch Experiments Co-products Linear Fitting.....	39
Figure 18 - Batch Experiments Co-products Linear Fitting.....	40
Figure 19 - Model fitting for Batch Experiments.....	41
Figure 20 - Model Fitting for Fed-batch Experiments.....	41
Figure 21 - Confidence Region for the Modified MM Model with Product Inhibition.....	43
Figure 22 - Stirring Power/Solids Concentration Scatter Plot.....	44
Figure 23 - Solids Above 97 g.L ⁻¹ Region Exponential Fitting.....	45
Figure 24 - Solids Bellow 97 g.L ⁻¹ Region Exponential Fitting.....	45
Figure 25 - Fed-batch Optimization for 360 h Process.....	47
Figure 26 - Fed-batch Optimization for 360 h Process Without Stirring Power.....	50
Figure 27 - Fed-batch Optimization for 360 h Process With Feeding Restriction.....	51
Figure 28 - Artificial Neural Network Errors - Poslin and Logsig Architectures.....	53
Figure 29 - Artificial Neural Network Errors - Poslin and Logsig Architectures.....	54
Figure 30 - Optimum Architecture Predicted Values.....	55

TABLE INDEX

Table 1 - Typical Composition of Sugarcane Bagasse Before and After Autohydrolysis..	5
Table 2 - Classification of Cellulose Hydrolysis Kinetic Models.....	7
Table 3 - Enzymatic Fed-Batch Hydrolysis of Lignocellulosic Biomass.....	12
Table 4 - Fed-Batch Feeding Profile.....	19
Table 5 - Particle Swarm Optimization Pseudocode.....	27
Table 6 - Co-products Linear Fitting.....	40
Table 7 - Models Parameters with 95% confidence intervals.....	42
Table 8 - Correlation Table for the Modified MM Model with Product Inhibition.....	42
Table 9 - Stirring Power Fitting Models.....	46
Table 10 - Unrestricted Feeding Policy.....	46
Table 11 - Unrestricted Feeding Policy Without Stirring Cost.....	49
Table 12 - Feeding Policy With Enzyme Addition Restriction.....	51

ABBREVIATIONS AND ACRONYMS INDEX

1G – First Generation

2G – Second Generation

ANN – Artificial Neural Network

CSS – Conductance and Capacitance Spectroscopy

FPU – Filter Paper Units

gbest – Global Best

LPS – Least Partial Square

MLP – Multilayer Perceptrons

MM – Michaelis-Mentem

MO - Modified

NF – Neuro-Fuzzy

NN – Neural Network

ODE – Ordinary Deferential Equation

PCA – Principal Component Analysis

PH – Pseudo-Homogeneous

PI – Product Inhibited

pbest – Personal Best

PSO – Particle Swarm Optimization

USB – Universal Serial Bus

UV – Ultraviolet

VIS - Visible

SUMMARY

Abstract.....	v
Resumo.....	vi
Figures Index.....	vii
Table Index.....	viii
Abbreviations and Acronyms Index.....	ix
1. Introduction And Objectives.....	1
2. Literature Review.....	3
2.1. Lignocellulosic compounds.....	3
2.2. Biomass Pretreatment.....	4
2.3. Lignocellulosic Biomass Hydrolysis.....	5
2.4. High Solids Enzymatic Hydrolysis.....	9
2.5. Biomass Hydrolysis in semi-continuous Operations.....	10
2.6. Optimal Control.....	12
2.7. Enzymatic Hydrolysis Fed-Batch Optimal Control.....	13
2.8. Online Fermentable carbohydrates Determination.....	15
3. Materials and Methods.....	18
3.1. Enzymatic Hydrolysis.....	18
3.2. Monitoring and Control System.....	19
3.3. Experimental Apparatus.....	20
3.4. Carbohydrates Determination.....	23
3.5. Model Fitting.....	24
3.6. Fed-Batch Optimization.....	29
3.7. Neural Network Optimization.....	32
4. Results and Discussion.....	35
4.1. Conductivity Monitoring.....	35
4.2. Full Array instrumentation.....	35
4.3. Batch and Fed-batch Experimental Data.....	38
4.4. Parameters Fitting.....	40
4.5. Stirring power/Solids Relation.....	44
4.6. Feeding Profile Optimization.....	46
4.7. Neural Network Calibration.....	52
5. Conclusions.....	57
6. Further Studies Suggestions.....	58
References.....	59

1. INTRODUCTION AND OBJECTIVES

The continuous demand growth for liquid fuels, alongside with the decrease of fossil oil reserves, unavoidable in the long term, induces investigations for new energy sources. A possible solution to substitute some liquid fossil fuels is the use of bioethanol, produced from renewable sources (NAIK et al., 2010).

In Brazil, a massive production of ethanol as automotive fuel occurred in the 1970s, when the government initiated a national program (Pró-Álcool) to reduce the dependency on foreign refined oil. The Pró-Álcool program had as main starting material sugarcane juice. This culture was intensified during this period, especially in southeast Brazil. The technology used in the program, called first generation (1G), was similar to the one utilized nowadays. But two thirds of the cultivated biomass, i.e. sugarcane bagasse or other lignocellulosic materials such as leaves, generates non fermentable substrates when the current process is applied (FREITAS & KANEKO, 2012).

Even though the biomass that is non fermentable via 1G processes may be used to generate other forms of energy (bioelectricity, production of syngas and so on), there is great interest in developing techniques capable of converting the carbohydrates from this material into bioethanol, thus generating more ethanol from each sugarcane mass unit (DANTAS et al., 2013).

Currently, large-scale 2G ethanol production still presents economic bottlenecks, . Among the most important technical hindrances is the scale up of the hydrolysis process to industrial application, in order to generate high product yields while keeping costs low (MODENBACH & NOKES, 2013).

This work intended to test and implement a softsensor architecture using Artificial Neural Networks, to predict the concentration of sugars in a bioreactor during the enzymatic hydrolysis of pretreated sugarcane bagasse using cellulases from a commercial cocktail. Besides, an algorithm based on optimal control theory was implemented, to define feeding strategies of substrate and/or enzymatic complex for the hydrolysis reactor.

It should be stressed that the main goal of this work is not to propose an optimal operational policy for a specific bioreactor, but rather to establish a consistent methodology to be applied in industrial plants. Besides, the experimental data that were used to fit models and to tune softsensors, and although the methodology may be consistent, the

final results hardly could be applied, directly, to industry-scale reactors.

Nevertheless, the algorithms presented here, using computational intelligence tools and applying advanced dynamic control theory, are expected, with modification, to be useful for further use in the biorefinery, thus contributing for the consolidation of the 2G industrial process.

2. LITERATURE REVIEW

2.1. LIGNOCELLULOSIC COMPOUNDS

Second generation biofuels are fuels produced from lignocellulosic substrates. These are fibers found in plants and vegetables. Their main function is to provide structural support, while assuring microbiological and chemical protection. The fractions of lignocellulosic materials are mostly composed by cellulose (32–55%), hemicellulose (19–24%), lignin (23–32%) and ashes (3–6%) (SANTOS et al., 2012).

Cellulose ($C_6H_{10}O_5$)_n is the most abundant polysaccharide in the fiber. Its ordered structure consists of several hundred glucose molecules (XU et al., 2013). The cellulose spatial conformation is determined by three main interactions. The first interaction is the β →1,4 glycosidic bond that unites a glucose to another glucose molecule through a covalent bond. This generates cellobiose, and this disaccharide is repeated throughout the polymer chain (ROCHA et al., 2011). The second interaction is among hydrogen molecules from the same chain and the third between adjacent chains. Due to these interactions, part of cellulose macromolecules can form a crystalline region, granting to the entire structure a high cohesiveness, and rendering it insoluble in water and several other solvents, and resistant to hydrolysis (SANTOS et al., 2012).

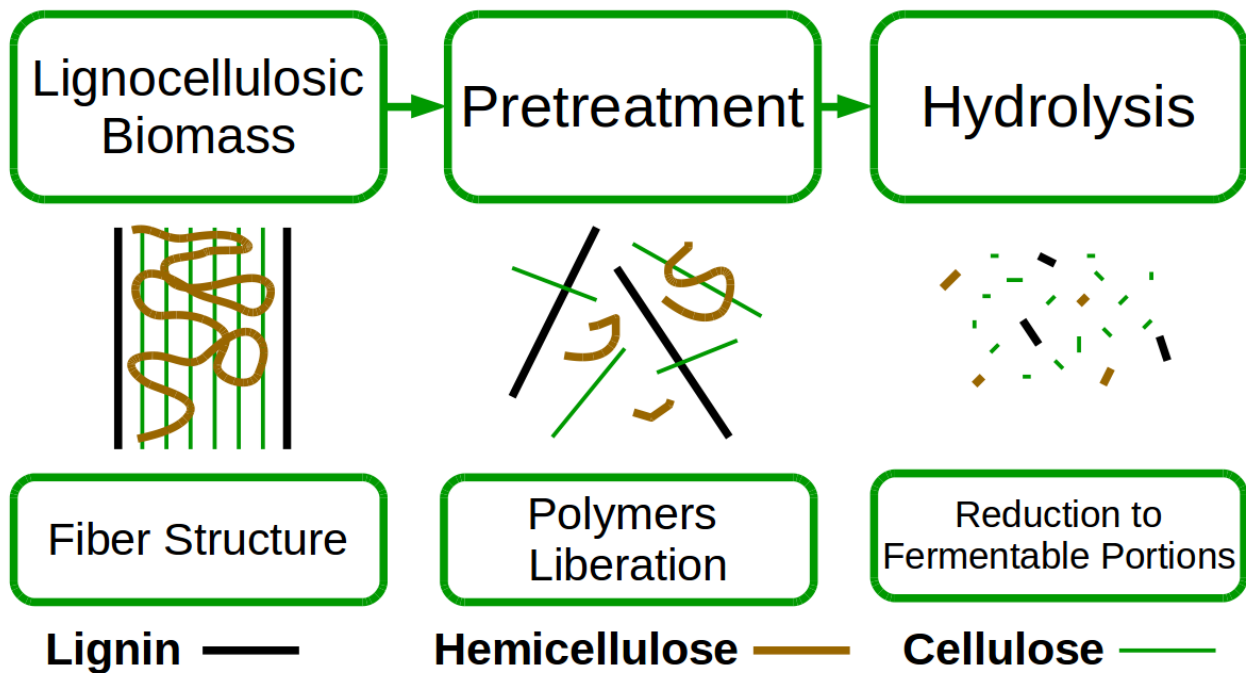
Hemicellulose differs significantly from cellulose. It is a heteropolysaccharide composed by hexoses (glucose, galactose and mannose), pentoses (xylose, the most abundant monomer, and arabinose), acetic acid, glucuronic acid and 4-O-methylglucuronic acid. The relation between these substances differs from vegetable to vegetable. This portion of the tissue does not form crystalline regions, thus it can be removed or hydrolyzed more easily than cellulose (CANILHA et al., 2012).

Lignin is formed by the polymerization of p-coumaryl alcohol, sinapyl alcohol and coniferyl alcohol. It is the second most abundant polymerer in the lignocellulosic biomass, and provides a barrier against foreign agents. Recalcitrance of the biomass is in great part due to this lignin barrier (ARANTES & SADDLER, 2011). In order to prevent this effect, a delignification procedure may be applied. From a biorefinery point of view, the recuperated lignin may be used in other processes (STEWART, 2008). Alternatively, its combustion will provide an extra heat source to the 2G process.

To produce ethanol from these lignocellulosic materials the structural

polysaccharides must be hydrolyzed, so that their monosaccharides (mostly pentoses and hexoses) become available to fermentative microorganisms. However, before the hydrolysis process, a pretreatment is required to separate and render cellulose and hemicellulose available to the hydrolytic action of the enzyme cocktail. A representation of the process is in Figure 1.

Figure 1 – Lignocellulosic Biomass Processing



(Source: author’s collection, adapted from: SANTOS et al., 2012)

2.2. BIOMASS PRETREATMENT

The pretreatment procedure destabilizes the lignocellulosic structure, making it more susceptible to further processing. This is achieved by increasing the material porosity, reducing cellulose crystallinity and removing lignin, to a certain degree. The entire procedure must be applied up to an intensity that generates an optimum platform for subsequent operations, while considering the formation of inhibitors and cost effectiveness (CHIARAMONTI et al, 2012).

Several methodologies are available for this process. Thus, the choice of the most adequate pretreatment depends on the feedstock, process plant design and economic situation (BANERJEE et al., 2010).

Among several available pretreatments, in this work special attention will be given to autohydrolysis, also known as hydrothermal pretreatment. This procedure requires a

pressurized reactor to maintain water in a liquid state at temperatures ranging from 150°C to 230°C, for different time periods. At these temperatures, biomass suffers cooking, increasing cellulose digestibility, while producing small amounts of inhibitors (KIM et al., 2009).

Another advantage of this technology is the absence of additional chemical compounds during the process, yielding a less toxic effluent than other alternatives. However, this pretreatment does not alter lignin to an extent that may render these molecules inactive in subsequent processes (MENON & RAO, 2012). A typical composition of sugarcane bagasse, for the most significant compounds, before and after the autohydrolysis process is presented in Table 1.

Table 1 – Typical Composition of Sugarcane Bagasse Before and After Autohydrolysis.

Compound	Raw Sugarcane Bagasse	Autohydrolysis Treated Bagasse
Cellulose (% w.w ⁻¹)	38.0	54.3
Hemicellulose (% w.w ⁻¹)	29.4	5.9
Lignin (% w.w ⁻¹)	21.7	24.8

(Source: Adapted from RODRIGUEZ-ZÚÑIGA et al., 2014)

2.3. LIGNOCELLULOSIC BIOMASS HYDROLYSIS

The pretreated biomass must be further hydrolyzed to provide fermentable fractions. At this stage, the polymers released by the pretreatment are converted to free monomers, readily available to fermentation. Two main technologies are used in order to hydrolyze lignocellulosic materials, using acid solution, generally sulfuric acid, or using enzymatic complexes (GAMAGE et al., 2010; SUN & CHENG, 2002).

Acid hydrolysis is usually divided in two groups, diluted and concentrated acid hydrolysis. In diluted acid hydrolysis, acid concentrations range from 1 to 3% w.w⁻¹, at high temperatures, 200–240°C. Due to the high temperature toxic compounds and inhibitors, such as furfurals and hydroxymethylfurfural, are generated after the degradation of pentoses and hexoses. This degradation does not only decrease the hydrolysis final yield, but the generated compounds are toxic to further production stages, such as the fermentation process (LIMAYEM & RICKE, 2012).

Concentrated acid is a more common process methodology. In this operation the acid concentration is high (90% w.w⁻¹) and, therefore, temperatures can be lower. Thus, this process generates a smaller amount of inhibitors. However, the utilization of such high acid concentrations is costly, and also generates a highly toxic effluent (SUN & CHENG, 2002).

This leads to the necessity for a more economically and environmental suitable process. One alternative is enzymatic hydrolysis. This sort of procedure yields high conversions, with fewer risks of producing toxic secondary products (LIMAYEM & RICKE, 2012). However, a high cost is inherent to this process, since, the compound itself has a high value and, with the current technology, direct enzymatic complex reuse is not feasible when using a soluble enzymatic complex (DANTAS et al., 2013).

To introduce enzymatic hydrolysis into the ethanol production route several research fronts are explored, among them: enzymatic complex improvement (KUPSKI et al., 2013); implementations of the second generation technology alongside the first generation process (FURLAN et al., 2012); utilizing high substrate loading; hydrolysis optimization modifying the feeding policy to the reactor in a fed-batch process (HODGE et al., 2009; CAVALCANTI-MONTAÑO et al., 2013).

2.3.1. Modeling Enzymatic Lignocellulosic Biomass Hydrolysis

To optimize the bioreactor design and operational conditions it is necessary to understand the kinetics that commands the interaction of the lignocellulosic material and the enzymatic complex. This study is difficult since several effects are reported among substrate and catalyst (SOUSA JR et al., 2011). To cope with such complexity, a large number of models are proposed to elucidate this process behavior.

Different approaches are used to model the process. A summary of them is presented in Table 2.

Analysis of Table 2 indicates that the model choice must be based on the goal to be achieved. As the model's phenomenological foundation increases, so does its complexity, generating the necessity for more specific data. However, for some reactive systems it may be unpractical—or even unfeasible—to measure all significant effects, necessary to validate more complex models. For a macro analysis of an industrial process, these details may not even be significant at all. Thus an adequate tradeoff between available data and model complexity must be sought.

Table 2 – Classification of Cellulose Hydrolysis Kinetic Models

Model Category	Features and Basis	Utility	Limitations
Nonmechanistic	Not Based in Enzyme/Substrate Interaction	- Good Data Adherence	- Does Not Enhance Phenomenon Understanding
Semimechanistic	Based in Enzyme/Substrate Interaction	- Good Data Adherence - Enhances Fundamental Understanding	- No Clarification on How Substrate Form Interferes in the Kinetics - All Enzymatic Activity Condensed in one Parameter
Functionally Based	Based in Enzyme/Substrate Interaction and Includes State Variables	- May Include Substrate Characteristics and Several Enzymes Activities	- Large Amount of Parameters Demanding More Experimental Data - Difficult Validation
Structurally Based	Based in the Substrate Morphological Information	- Generates Understanding of How the Substrate Characteristics Affect Hydrolysis	- Model Composition is Difficult - Demands Specific Data

(Adapted from Zhang & Lynd, 2004)

A good equilibrium point in this tradeoff is the utilization of semi-mechanistic models. Models of this category reflect some—at least rough—understanding of the phenomena occurring in the system, though only using relative simple data, such as product concentration throughout time, for model fitting and validation. This class of model is generally applied for optimization and designing industrial reactors (CARVALHO et al., 2013).

The most popular semi-mechanistic models for enzymatic reactions are derivations of Michaelis-Menten's (Michaelis & Menten, 1913). However, Michaelis-Menten model is based on mass action laws valid for substrates (and products) in the fluid (liquid, in this case) phase. This is not true for the specific case of lignocellulosic hydrolysis, since most of the substrate is solid. The excess substrate to enzyme condition ($[S] \gg [E]$), necessary to the quasi-steady state condition, is also never achieved, since the fraction of cellulose available to hydrolysis is not high enough. This derives from the fact that hydrolysis occurs in a heterogeneous medium, and the reaction is occurring on the substrate surface, so the enzyme must first diffuse to the reactive site to be able to act (BANSAL et al., 2009).

Nevertheless, literature has shown that Michaelis-Mentem models may be suitable to fit experimental results of the hydrolysis of lignocellulosic materials, despite the lack of physical-chemical background. Yet, in order to use this type of model some assumption regarding the substrate solid state must be established. Two options are available in the literature: using a pseudo-homogenous assumption for the solid substrate (Equation 1). Or using a modified form of the model, which assumes that the soluble enzyme attacks the solid substrate, but with negligible changes of the substrate initial concentration (Equation 2); the soluble enzyme has to absorb (and desorb) from the solid substrate. The concentration of enzyme absorbed on the substrate must be much smaller than the amount free in the medium ($[E] \gg [E_{ads}]$) (CARVALHO et al., 2013).

$$v = \frac{k \cdot [E] \cdot [S]}{(K_m + [S])} \quad \text{Equation 1}$$

$$v = \frac{k \cdot [E] \cdot [S]}{(K_m + [E])} \quad \text{Equation 2}$$

Where, v is the reaction rate, k is the enzyme turnover number, $[E]$ is the enzyme concentration, $[S]$ is the substrate concentration and K_m is the Michaelis-Mentem half-saturation constant.

Both models are showed to be able of fitting hydrolysis data. However, they do not account for inhibitors present in the process. Bezerra & Dias (2004) showed that a pseudo-homogenous model with competitive inhibition by the product was the most suitable model in this case, as other effects that may reduce hydrolysis rates, such as nonproductive cellulase binding, enzyme jamming and enzyme deactivation were not so significant, according to these authors. Following this approach, Equation 1 can be modified into Equation 3.

$$v = \frac{k \cdot [E] \cdot [S]}{K_m \cdot \left(1 + \frac{[P]}{K_{ic}}\right) + [S]} \quad \text{Equation 3}$$

Where K_{ic} is the competitive inhibition constant. Even though this is a rather simplified model, it is expected from the literature results that this structure may hold for the conditions that will be studied in this work.

The same consideration of competitive inhibition can be applied to Equation 2, to generate a modified Michaelis-Menten model with product inhibition.

$$v = \frac{k \cdot [E] \cdot [S]}{K_m \cdot \left(1 + \frac{[P]}{K_{ic}}\right) + [E]} \quad \text{Equation 4}$$

2.3.2. Enzymatic Complex

Due to the high complexity of the lignocellulosic material, the enzymatic catalyst used for biomass hydrolysis is not composed by only one active protein, but by a congress of several molecules, each interacting with a portion of the substrate.

The enzymes that interact with cellulose to produce glucose are denominated cellulases. Cellulases are enzymatic complexes that may be produced by fermentation of filamentous fungi from the genre *Trichoderma*, *Aspergillus* and *Penicillium* (WYMAN, 2003).

Cellulases are divided in three main groups. Endoglucanases (endo-1,4- β -glucanase) work in the amorphous region of the cellulose molecule and binds randomly, liberating reductive ends in the chain. Celobiohydrolases (exo-1,4- β -glucanase) act in the reducing and non-reducing ends of the chain, both e natural ones, and on the ones generated by Endoglucanases. The last group is composed by β -glucosidases and its function is to hydrolyze cellobiose into glucose (THONGEKKAEW et al, 2008). Other enzymes may be used as additives to enhance the performance of the cocktail. Oxidases such as lytic polysaccharides monooxygenases are one example (HORN et al., 2012).

Residual hemicellulose, that was preserved in the solid substrate after the pre-treatment of the biomass, can be hydrolyzed by the action of a group of enzymes know as Hemicellulases. Among them are: endoxylanases, β -xylanes and α -L-arabinofuranosidase, among others (JORGENSEN et al., 2007).

All these enzymes are commonly found in commercial cocktails, although the exact composition of such complexes is not disclosed..

2.4. HIGH SOLIDS ENZYMATIC HYDROLYSIS

The so called C6 liquor, essentially glucose for further fermentation (with *Saccharomyces cerevisiae*), is the output of the enzymatic bioreactor, where cellulose

hydrolysis occurs. For the economics of the overall processes, it is very important that glucose is yielded at high concentrations, thus reducing the amount of water in the solution. Ideally, for sugar cane mills, the target should be minimizing the energy demand by reaching glucose concentrations as close as possible to the sugarcane juice's, approximately 180 g.L^{-1} (FERNANDES, 2003). Either if the C6 liquor is used in separate fermenters or if it is mixed with the sugarcane juice, a concentrated C6 liquor will reduce the demand of heating power in the global process (DIAS et al., 2012; FURLAN et al., 2012).

Thus, a high solid consistency (load of substrate within the reactor) is necessary, generating a more concentrated carbohydrate solution at the end of the process. As previously mentioned, a more concentrated final product would enable the addition of the 2G stream to the 1G's, before the fermentation (HUMBIRD et al., 2010), without (or with minimal) demand of evaporators after the hydrolysis reactor. High-solids loadings also generate economical advantages since the operational volume will be lower than with low-solids operation, resulting in less energy to heat or cool the reactor. Disposal treatment costs would be lower too, due to the reduction of water usage (HODGE et al., 2009).

High Solids processes are those where the ratio of solid material to aqueous phase is such that very little free liquid is present (HODGE et al., 2009). As water becomes sparse within the reactor two main issues arise. Water is first and foremost necessary in order to provide a medium in which the chemical reaction will take place. At high solids content, mass transfer becomes an issue, since the enzyme will be hindered to reaching its reactive site (MODENBACH & NOKES, 2013).

The second issue is the reactive medium apparent viscosity. Water dilutes the solids inside the reactor, effectively decreasing viscosity, and increasing the lubricity between the particles. A larger lubricity decreases the required shear rate to agitate the reactor. A smaller agitation necessity leads to smaller power consumption. Therefore, at high solids rates, reactor mixing becomes an issue, due to the high power demanded (KRISTENSEN et al., 2009). Thus, it would be interesting to have a reactor operational policy that would bypass such conditions.

2.5. BIOMASS HYDROLYSIS IN SEMI-CONTINUOUS OPERATIONS

Biomass hydrolysis in fed-batch processes appears as a promising strategy since adverse conditions of a standard batch are avoided. A process policy where substrate is

fed into the reactor continuously avoids the necessity of beginning the process with high solid loadings, facilitating the system homogenization. Furthermore, in fed-batch process, when compared to the same process done in a standard batch process, the conversion and productivity is higher, since smaller solid loadings diminish inhibitions, especially enzyme/substrate inhibitions (HODGE et al., 2009).

Studies for the optimization of fed-batch processes may begin by promoting batch hydrolyses under high-solids concentrations, when stirring and mixing in the tank may become a problem (HODGE et al., 2008). After the reactor model is consolidated, alterations are made in order to contemplate the feeding flow (HODGE et al., 2009).

Most of the published studies deal with spreading the initial substrate load evenly during the batch time, and do not propose optimum profiles (CHANDRA et al., 2011; GUPTA et al., 2012). This implementation does not optimize the system, and may not maximize its performance. Optimal control theory (dynamic optimization) may be applied to maximize productivity and minimize the utilization of enzymatic complex (CAVALCANTI-MONTAÑO et al., 2013). A summary of previous literature results in the subject is presented in Table 3.

Table 3 brings important points to the discussion. The work of Chandra et al. (2011) is the only presented research that does not demonstrate an improvement with the fed-batch system when compared with a standard batch. This work also is the only one that does not alter enzyme complex concentration throughout the process, indicating that there can be a relation between the enzyme feeding profile and fed-batch/batch improvement.

Another important characteristic is that none of the cited works considers the power demands for stirring within the reactor. The papers do not consider how the solids concentration will influence the reactor operation cost, and when the solid concentration is considered, the value is related to the reactor operational range, and not related to some index indicating the performance of the process. Nevertheless, as it will be shown further, it is imperative to consider the agitation power, and how it is changed by solids concentration, for the optimization of the process.

Table 3 – Enzymatic Fed-Batch Hydrolysis of Lignocellulosic Biomass

Paper	Manipulated Variables	Control Policy	Conclusion
Hodge et al, 2009	Solids and Enzyme Feeding	Maintain Solids Concentration to a Set-point of 15% w.w ⁻¹	80% Total Cellulose Conversion in a Process Equivalent to Batch With 25% w.w ⁻¹ Initial Solids
Morales-Rodriguez et al., 2010	Solids and Enzyme Feeding	Proportional-Integral Control to Maintain Solids Concentration to a Set-point and Minimize Enzyme Addition	Reduction of 107% in Enzyme Addition
Chandra et al., 2011	Solids Feeding	Fixed Feeding Scattered Through the Process	No Appreciable Difference Between Batch and Fed-Batch Process
Gupta et al., 2012	Solids and Enzyme Feeding	Fixed Feeding Scattered Through the Process	Fed-Batch Conversion 56% Better Than Equivalent Batch Process
Cavalcanti-Montaño et al., 2013	Policy 1: Solids Feeding Policy 2: Solids and Enzyme Feeding	Policy 1: Optimal Control Policy 2: Control to Maintain High Hydrolysis Velocity	200 g.L ⁻¹ Final Carbohydrates Concentration – Improvement from the Batch for High Enzyme Prices

2.6. OPTIMAL CONTROL

The optimal control problem (or dynamic optimization) consists in, basically, finding control variables optimum profiles (several decisions dynamics), control parameters or project variables values (static variables) and possibly the process final time that maximizes (or minimize) a performance scalar (objective function or cost function) (RIBEIRO & GIORDANO, 2005; RAMIREZ, 2004). The direct formulation of the optimal control problem is as follows (SRINIVASAN et al., 2003):

$$\min_{(\underline{u}(t), \underline{p}, t)} J(\underline{u}, \underline{p}) = \psi(x(t_f), \underline{p}, t_f) \quad \text{Equation 5}$$

Subjected to:

$$\dot{\underline{x}} = f(\underline{x}(t), \underline{u}(t), \underline{p}, t) \quad \underline{x}(t_0) = x_0 \quad \text{Equation 6}$$

$$\underline{g}(\underline{x}(t), \underline{u}(t), \underline{p}, t) = 0 \quad \text{Equation 7}$$

$$\underline{S}(\underline{x}(t), \underline{u}(t), \underline{p}) \leq 0 \quad T(\underline{x}(t_f)) \leq x_0 \quad \text{Equation 8}$$

By minimizing, or maximizing, the functional, or cost function, J under the constraints and weights given by the other equations an optimum profile for the control variable may be calculated (RAMIREZ, 2004).

Where J is the functional, or cost function, $\underline{x}(t)$ is the state variables vector, and x_0 is the, usually known initial conditions, $\underline{u}(t)$ is the control variable profile throughout time, \underline{g} is the equality constraint vector, \underline{S} is the inequality constraint vector and \underline{p} are static decision variables.

There are several methods to calculate the optimum solution. The solution method varies with how the state and input variables are handled, and how the numerical solution is carried out. The functional presented in Equation 5 may be optimized in a direct approach, by using an optimization algorithm, or indirect approach, by using methods based in variational calculus such as the Pontryagin's Minimum Principle and the principle of optimality of Hamilton-Jacobi-Bellman (SRINIVASAN et al., 2003).

A simple method for solving the optimal control problem stated (Equations 5–8) is the sequential approach. In contrast to indirect approaches, in this direct method no analytical differentiation is needed and it is an adjoint-free computation, i.e. no adjoint variables (Lagrange multipliers) has to be calculate. In this method however, the control vector, $\underline{u}(t)$ must be parameterized using a finite set of parameters—the actual decision variables. Though this method is easy to implement, it tends to be slow, especially when inequality path constraints are included in the problem. (SRINIVASAN et al., 2003).

2.7. ENZYMATIC HYDROLYSIS FED-BATCH OPTIMAL CONTROL

It should be stressed that the definition of the functional, or cost function, is a key step to have a well-posed optimal control problem. Defining reasonable criteria to evaluate the “optimality” of a specific solution in real life is probably the most challenging task for the process engineer that is implementing optimal control algorithms.

In the special case of lignocellulosic hydrolysis, some possible performance indexes are: productivity per enzyme mass, fermentable carbohydrates conversion, final

carbohydrates concentration, some economical index related with the operational cost of the bioreactor with the selling price of bioethanol. The dynamic control variables may be the mass inflow of substrate and of enzymatic complex.

Most optimal control techniques presented in the literature for biomass hydrolysis are open loop, no method for information feedback is used. That is, the optimal policies are previously computed, assuming that the real process will not deviate greatly from the model predictions. Thus, disturbances originated from several sources, such as substrate composition variations or errors in secondary control systems, are not corrected by the control software (UPETRI, 2013). To consider these variations it is necessary to close the control loop, enabling the automatic update of control profiles based on the current state and future possibilities.

The feedback of data gives the control layer capabilities for dealing with uncertainties, not considered in the internal models. Previously determined kinetic parameters may then be re-estimated, and optimum trajectories of the system, recalculated. The feedback may generate a better performance when comparing to open optimization. However, a closed-loop control mesh may render the system more sensitive to external variations. This comes from the fact that, to maintain the system optimized, the controller distributes the error into the controlled values by intensifying activations densities. This effect generates a stress in the component, since more activations are necessary (NAGY & BRAATZ, 2004).

Commonly, the update of optimal profiles for fed-batch processes is translated into changes in the feeding streams to the reactor. This is especially the case when temperature is not an adequate variable to be manipulated, following profiles that change with time: certainly, this is not a desirable strategy for an enzymatic reactor, since the catalytic action of the enzymes is restrict to narrow ranges of temperature. Essentially, this kind of reactor will be operated isothermally, in a temperature where the enzyme activity is high, while thermal inactivation is not significant. Although, this approach may be improved (considering thermal profiles during operation of the reactor), in this work the reactor will be isothermal (the temperature closed loop feedback control runs in standalone feature, with a fixed set point).

Besides temperature, other secondary variables may be manipulated by the dynamic control algorithm. One example is the agitation rate.

2.8. ONLINE FERMENTABLE CARBOHYDRATES DETERMINATION

In the hydrolysis of the cellulose fraction of the biomass, the desired products are free carbohydrates, especially glucose. Therefore, to optimize this compound final concentration, a methodology capable of predicting concentrations of this substance online is necessary. Several methods can be applied to quantify them, ranging from titration and colorimetric techniques to chromatographic analysis (SLUITER et al., 2010).

Nevertheless, these techniques are used in laboratory scale, demanding qualified operators and a relatively long time (DEMARTINI et al., 2011). Therefore, usual analytical techniques are not suitable to online monitoring, and more suitable methods must be developed, able to be used within an automated supervision/control framework.

A possible alternative to monitor fermentable carbohydrates is the utilization of soft sensing to infer the state of the system. In a softsensor, a set of measurements, obtained from different sensors, are the input for a model (usually empirical, black box) whose output is the inference of the variable of interest. Although extrapolation is not expected to be accurate with this kind of model, the accuracy and precision of the predictions must hold when a set of input values is not contained in the original experimental data (but is within the range of the data used for tuning the softsensor). Among the most popular soft sensing algorithms are: Principle Component Analysis (PCA) combined with Least Partial Square (LPS) regression; Artificial Neural Networks (ANN); and Neuro-Fuzzy systems (NF) (KADLEC et al., 2009).

Artificial Neural Networks (ANNs) are mathematical models inspired by the mechanism that the human brain uses to handle information. One important application of ANNs is pattern recognition. Among several types of ANN architectures, the multilayer perceptrons (MLP) can be highlighted. In this architecture each artificial neuron is connected to all the neurons in the following layer, the input for each neuron is multiplied by a weight value and then it is introduced into a transfer function. The network composition is carried by a training stage using an optimization method to minimize the error between the model output and the experimental value, using independent test data sets (not applied in the tuning of the ANN parameters) to avoid overfitting. After training, the network may be applied to predict the value of the monitored variable from the primary, directly measurable, variables (DEHURI & CHO, 2009).

2.8.1. Torque Measurement

Torque is an important variable when analyzing the rheometry of a solution or suspension. Usually, torque measurement is done off-line: a sample of the medium is loaded in a bench rheometer (EHRHARDT et al., 2010).

In studies that monitor rheometry throughout the enzymatic hydrolysis process, a clear decrease in the torque demanded to agitate the medium is observed when the solids in the reactor are hydrolyzed (SAMANIUK et al., 2011) However, these authors did not measure the torque online. Using a system capable of monitoring the torque throughout the process may enable solids monitoring, and this measured data can be used in the soft sensor.

2.8.2. Visible and Ultraviolet Spectroscopy

An analytical online system, capable of analyzing the supernatant optical properties, alongside the hydrolysis reactor, can uncover new behaviors of the hydrolysis kinetics. Specially the presence of inhibitors of the enzyme complex within the reactor may be detected.

This idea is supported by the fact that lignin absorbs electromagnetic radiation strongly in the ultraviolet region. Some methodologies use this characteristic in order to ascertain lignin contents in the biomass (NREL, 2008; GOUVEIA et al., 2009; KLINE et al., 2010).

Thus, an instrumentation capable of measuring lignin, as well as other possible analytes, can be feedback into the controller unit in order to generate the input of the soft sensor, and provide information (including inhibitors concentrations) to re-parametrize the kinetic model used by the optimal control algorithm.

2.8.3. Conductance/Capacitance Spectroscopy

Conductance and Capacitance Spectroscopy (CCS) is based on the generation of alternating electrical fields in the media (inside the reactor, in our case). Thus, the CCS sensor is an *in situ* measuring device. Under certain frequencies, some groups of molecules are polarized. This polarization changes the dielectric constant of the medium. This can be measured as variations in the conductance, the capacity of the medium to allow an electrical current to pass through itself, and capacitance, the capacity of a medium to store electrical charge (VOJINOVI et al., 2006).

CCS has been recently reported for monitoring the hydrolysis of lignocellulosic

material by BRYANT et al., 2013 who observed a linear correlation between capacitance the contents of solids inside the reactor.

Therefore, an instrument of this sort can be used to aid the monitoring of the reactor, either as a standalone instrument or as a source of input signals to the soft sensor layer.

3. MATERIALS AND METHODS

3.1. ENZYMATIC HYDROLYSIS

Bagasse was donated by Usina Ipiranga S/A (Descalvado, SP), and it is the product of milling sugar cane used to extract the high carbohydrate content juice from this vegetable.

Batch and fed-batch enzymatic hydrolysis were realized utilizing hydrothermally pretreated sugar cane bagasse. The pretreatment was carried out in pressurized reactor, with a maximum pressure of 200 psi, at 200 RPM. The reactor was loaded with 0.010 grams of dry bagasse per milliliter of reactor ($10\% \text{ w.v}^{-1}$) and then programmed to reach $195\text{ }^{\circ}\text{C}$ and hold this temperature for 10 min. The pretreated bagasse was then dried in kiln for 24h at $60\text{ }^{\circ}\text{C}$.

The batch experiments were realized using $10\% \text{ w.v}^{-1}$ of dry pretreated bagasse suspended in 4.80 pH and 50 mM citrate buffer and 50°C (Wang et al., 2012). The hydrolysis was carried out in agitated vessel containing 3 L of reactive media in a 5 L container. The reactor was stirred at 470 RPM by a pair of Rushton impellers, both equally distributed between the vessel bottom and the liquid surface. Temperature inside the reactor was maintained using a thermostatic water bath set to $50\text{ }^{\circ}\text{C}$. The total batch time was 48 h and manual analysis were performed at 0.0, 0.5, 1.0, 2.0, 4.0, 6.0, 12.0, 24.0, 36.0 and 48.0 h.

The enzymatic complex used was Cellic Ctec 2[®] donated by Novozymes Latin America (Araucária, PR). In the batch experiments, 1.04 g (13.84 mL) were added, this mass is equivalent to a loading of $10\text{ FPU.g}_{\text{Bagasse}}^{-1}$, which is the operational load in studies within the research group. Filter Paper Unity (FPU) is the unit used in order to measure cellulase hydrolysis potential.

The fed-batch experiments were performed with similar conditions to those of batch experiments, 4.80 pH and 50 mM citrate buffer and 50°C . However, the substrate and enzymatic complex were not added in the beginning of the process, but, however, fed to the reactor following a feeding profile, presented in Table 4. The experiments lasted for 6h. The substrate feeding was carried out with a solids concentration of 40% in the inlet flow. The reactor initial volume was 3 L and was filled until 3.5 L.

Two experiments were performed for each strategy. Manual samples were taken 2

minutes before and 2 minutes after each feeding instant.

Table 4 – Fed-Batch Feeding Profile

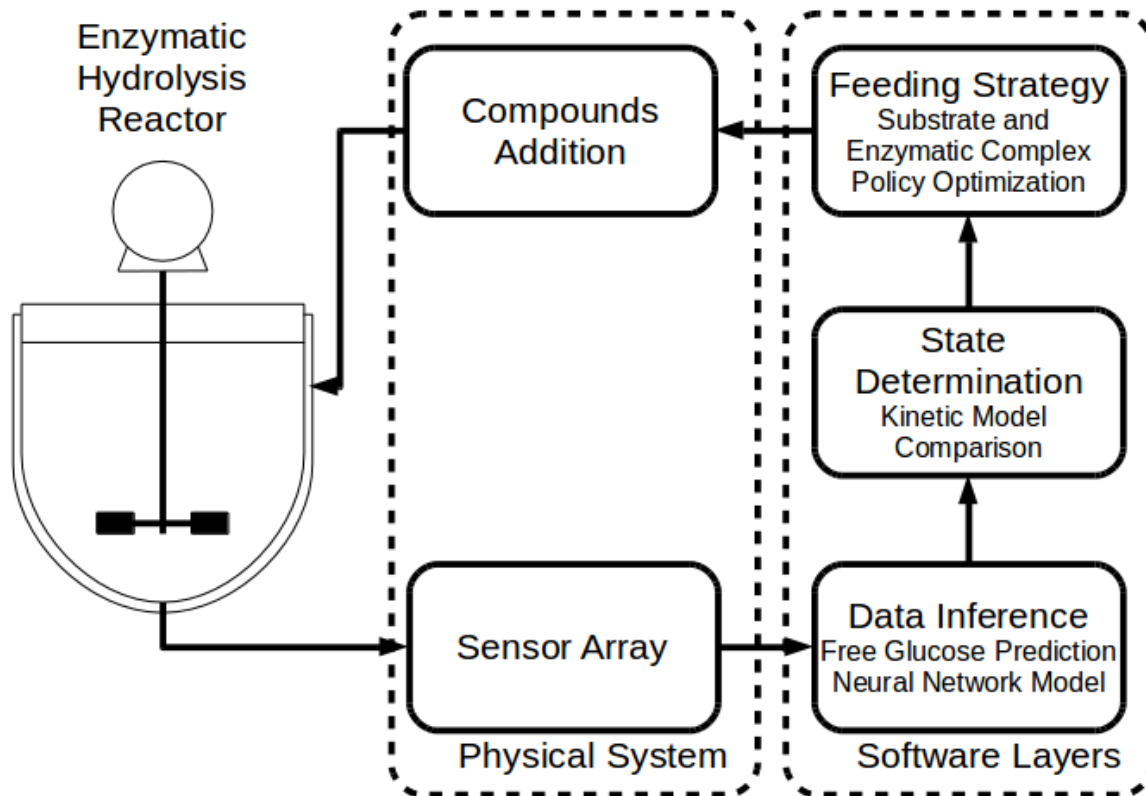
Time (h)	Solids Feeding (g)	Accumulated Solids (g)	Enzyme Feeding (g)	Accumulated Enzyme (g)
0.00	191.02	191.02	0.31	0.31
0.50	0.51	191.54	0.23	0.54
1.00	5.50	197.04	0.56	1.10
1.50	1.30	198.34	0.33	1.43
2.00	10.83	209.17	0.38	1.81
2.50	8.09	217.26	0.32	2.13
3.00	6.93	224.19	0.14	2.28
3.50	49.25	273.45	0.11	2.38
4.00	10.74	284.19	0.43	2.82
4.50	6.35	290.54	0.22	3.03
5.00	13.37	303.91	0.08	3.11
5.50	0.35	304.25	0.00	3.11

3.2. MONITORING AND CONTROL SYSTEM

This work proposes the dimensioning and construction of a system capable of monitoring, translating the data from a sensor array into a product concentration prediction, evaluating the reaction state and optimizing further activations to maximize the process efficiency. A schematic of how the system works is presented in Figure 2.

Further explanations on how the systems interact are contained in the following items.

Figure 2 - Monitoring and control system



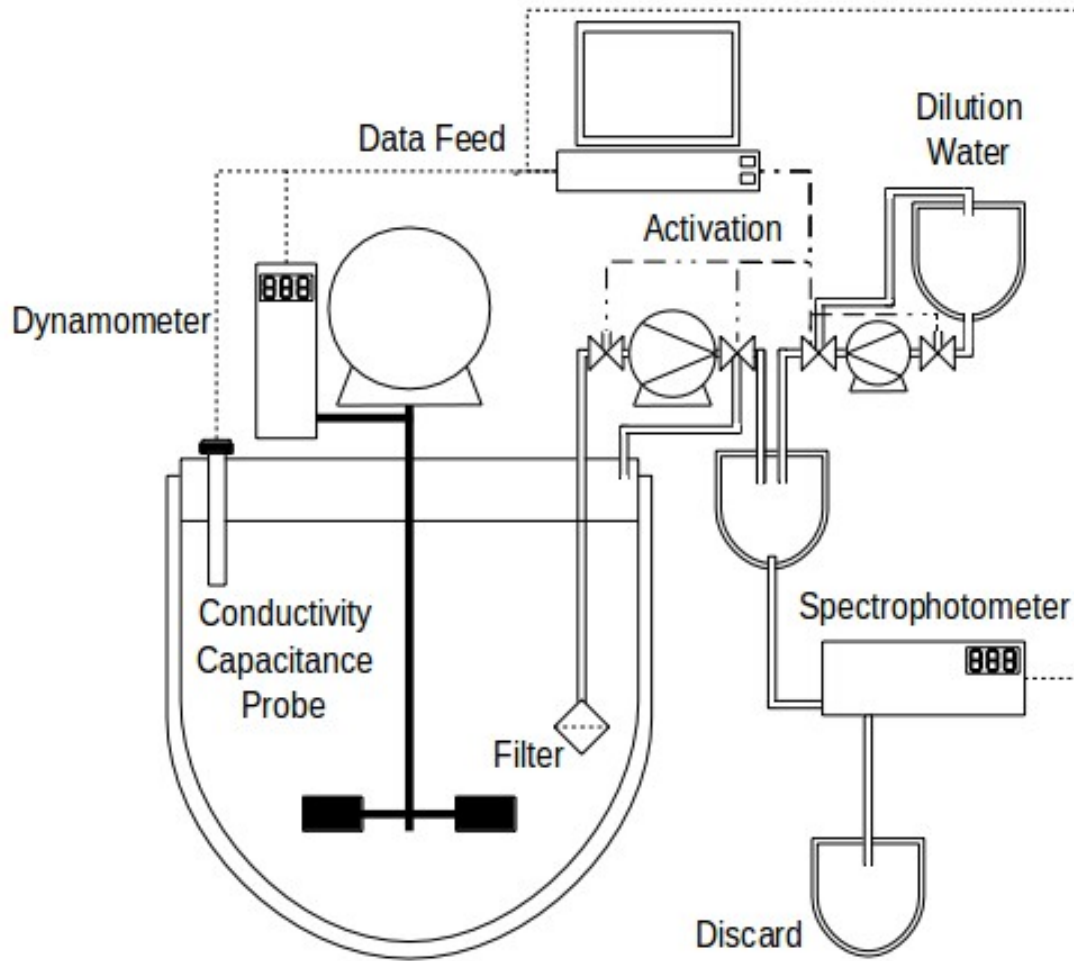
(Source: author's collection)

3.3. EXPERIMENTAL APPARATUS

The reactor where the hydrolysis happens possesses an instrumentation array with the purpose of monitoring the free glucose concentration inside the reactive media at any given time during the hydrolysis process. The sensors measurements are relayed to a server that decodes the information, converts to the root unit of measurement when necessary and stores the data.

Figure 3 presents a scheme of the system sensors.

Figure 3 - Sensor array coupling



(Source: author's collection)

3.3.1. Torque Measurement

The torque measurement is achieved using digital dynamometer coupled to the stirring shaft. The electric motor is above a ball bearing mount, thus the engine is free to roll in its own axle. By coupling a dynamometer perpendicularly to a rod fixated in the ball bearing a force is measured. This force is proportional to the amount of energy necessary to agitate the reactive media. To convert the straight force into stirring power, Equation 9 was used.

$$P = T \cdot \omega \quad \text{Equation 9}$$

Where P, is the power necessary for the stirring motion, T is the torque measurement itself and ω is the axle angular velocity. Torque may be substituted by the

variables in Equation 10.

$$T = F \cdot L \quad \text{Equation 10}$$

Where F is the force provided by the dynamometer and L the distance of the dynamometer coupling to the center of the agitation axle. Further modifications are provided by Equation 11.

$$\omega = 2 \cdot \pi \cdot N \quad \text{Equation 11}$$

Where N is the rotation frequency, results in a simplification to convert the force measured by the dynamometer into stirring power presented in Equation 12.

$$P = 2 \cdot \pi \cdot F \cdot L \cdot N \quad \text{Equation 12}$$

This instrument relays data through a serial connection to a server under a RS-232 protocol. The server receives this information through a universal serial bus (USB) port and handles the data in a software layer inside a Python console. This measurement was made at every minute of the batch.

3.3.2. Supernatant Sampling and Scan

The supernatant optical properties was measured by an analytical line once an hour. The supernatant sampling begins with the filtration of the reactive media by a pumice stone filter. The driving force for the filtration was provided by a peristaltic pump. Part of the filtrated supernatant, 0.2 mL, was destined to a dilution vessel. The dilution was accomplished by a series of valves and a peristaltic pump. The dilution line worked iteratively, adding 4.0 mL per iteration, and the sample dilution necessity was assessed by the last scan, updating itself automatically.

After the dilution, the prepared sample was injected into a flow cuvette inside the spectrophotometer. With the sample properly contained, 20 scans ranging from 190 to 1100 nm was performed. This range comprehends the ultra violet and visible region of the electromagnetic spectrum. The data generated by the scans were transmitted to the server by a serial connection, under a RS-232 protocol, and the server received the information through a USB port and decoded by a software layer ran in a Python console.

At the end of the scans, dilution water was injected into the cuvette to clean it. After the cleaning period, only water was added to the cuvette and 5 scans were performed to establish a baseline for the next series of scans.

The automation of sampling system was accomplished by a physical computational device for data acquisition called Arduino. The Arduino board is an open hardware platform capable of generating electronic outputs or reading inputs in a standalone method or as a slave for a server (BANZI, 2009). The signals to change the controller states are generated by a software layer coded and run in a Python console.

3.3.3. Conductivity and Capacitance Measurement

The conductivity and capacitance measurements was performed by a single probe connected to a preamplifier and transmission module Fogale Nanobiotech. The frequency used was 382 kHz.

3.3.4. Enzymatic Hydrolysis Monitoring Through Conductivity

Small-scale studies were carried out to assess how the conductivity changes inside the hydrolysis media and evaluate this methodology as a tool to monitor hydrolysis inside the reactor before adding this instrumentation a larger reactor. Three small-scale batch experiments were conducted in a 500 mL reactor, with conditions similar to the large-scale experiments. Citrate buffer at 4.80 pH and 50 mM, 10% w.v⁻¹ dry bagasse, 50 °C and adding 0.17 g of enzymatic complex. In these experiments, the probe relayed its data through a serial RS-232 connection and the decoding was achieved by the proprietary software.

In the larger scales, the rest of the instrumentation was applied, however when using the capacitance/conductivity system inside the 3L reactor the acquired data by this probe was relayed to the server through a 4 to 20 mA connection. The signal was read by the data acquisition module Arduino Mega through two analog input ports, and then the data was relayed to the server via serial RS-232 connection.

3.4. CARBOHYDRATES DETERMINATION

Glucose determination was carried out manually at the offline sampling periods described in the Item 3.1. The analysis itself was performed via glucose oxidase/peroxidase enzymatic determination kit (Doles; Goiânia, GO, Brazil) and High-Performance Liquid Chromatography (HPLC).

The samples were withdrawn from the reactor by filling a 2 mL vessel with reactive media. The container was centrifuged for 7 min at 10,000 RPM. 0.5 mL of the supernatant was combined with 0.1 mL of sodium hydroxide 0.2 N to maintain storage preservation.

HPLC was used to determinate glucose, xylose and cellobiose concentrations. The samples were analyzed in Shimadzu SCL-10A chromatograph using refraction index detector RID10-A, Animex HPX-87H Bio-rad, using as mobile phase sulfuric acid 5 mM at a flow of 0.6 mL.min⁻¹. The samples were compared to previously established standards (NREL, 2008).

Enzymatic kit analysis was used to check HPLC glucose concentration. The analysis occurred by combining 10 µmL of the prepared sample and 1 mL of the enzymatic analysis complex, incubating the mixture at 37°C for 5 min and measuring the absorbance at 510 nm. The measured absorbance was compared to a standard curve of glucose determined with the kit in the same manner that the sample is analyzed. All analyses were performed in triplicates.

3.5. MODEL FITTING

The glucose concentrations, generated by both the batch and fed-batch experiments, were used to estimate the coefficients for the 4 models presented in item 2.4.1. In order to calculate the error between model and experimental data, simulated glucose concentration were obtained by integrating th following components balance.

$$\frac{dS}{dt} = \frac{F_{Substrate}}{V} - v - \frac{[S] \cdot F_{Substrate}}{V} \quad \text{Equation 13}$$

$$\frac{dP}{dt} = v - \frac{[P] \cdot F_{Substrate}}{V} \quad \text{Equation 14}$$

$$\frac{dE}{dt} = \frac{F_{Enzyme}}{V} - \frac{[E] \cdot F_{Enzyme}}{V} \quad \text{Equation 15}$$

$$\frac{dSol}{dt} = \frac{F_{Substrate}}{V} - \frac{v}{1.10} - Xyl \cdot v - Cell \cdot v - \frac{[Sol] \cdot F_{Substrate}}{V} \quad \text{Equation 16}$$

$$\frac{dV}{dt} = F_{Substrate} + F_{Enzyme} \quad \text{Equation 17}$$

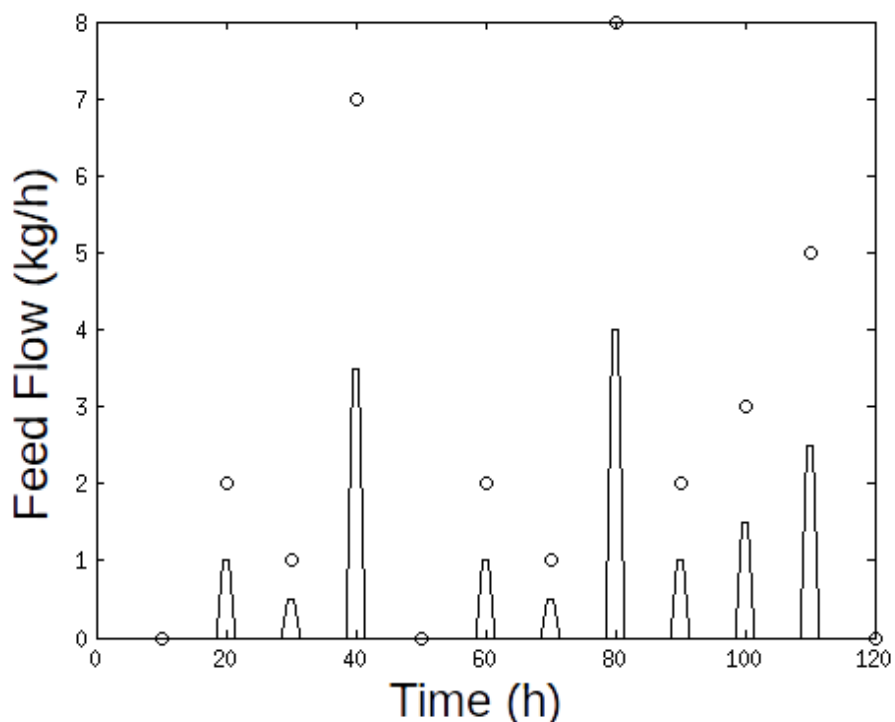
Where $[S]$ is the substrate concentration, $F_{Substrate}$ is the inlet flow of substrate, v is the enzymatic velocity, $[P]$ is the product concentration, $[E]$ is the enzyme concentration, F_{Enzyme} is the inlet flow of enzyme, $[Sol]$ is the non-reactive solids concentration, Xyl and Cell are stoichiometric empirical rates for xylose and cellobiose.

The stoichiometric rates were adjusted with the data provided by the

chromatographic analysis. The xylose and cellobiose concentrations are estimated from a linear fitting of these compounds and the glucose concentration. This procedure is carried separately for the batch and fed-batch experiments.

To avoid inconsistencies in the numerical solving of the model, the feeding profile cannot be a discrete vector with punctual in certain time instants. Therefore, the vector was interpolated to a continuous function throughout the time domain. A representation of this interpolation is presented in Figure 4.

Figure 4 - Interpolation Example



(Source: author's collection) (Where: Discrete feedings (kg) at certain time instants were approximated to a continuous flow ($\text{kg}\cdot\text{h}^{-1}$))

In the Fig. 4, the blue circles represent the discrete values (optimized feeding vectors) and the blue solid line represents the generated continuous function. The interpolation algorithm behaved equally for the bagasse and enzymatic complex input profiles.

The numerical method used to integrate the differential system was a Runge-Kutta 4th order with variable step. Particle Swarm Optimization (PSO) algorithm was used to fit the parameters.

PSO minimizes the average quadratic error between the system output and the

experimental value (cost function chosen) by generating a series of particles. These particles are scattered in a multidimensional space, with as many dimensions as there are parameters to be optimized, in this case a 3 dimensions space. A velocity in each dimension is attributed to the particle. Since the dimensions are the parameters to be optimized, one particle position is tested inside the model to evaluate its fitting. If the new fitting is better (smaller error) than a previous one found by the same particle (Personal Best) the new position is attributed as a new best particular position. The fitting value is also compared to a Global Best, which is the best value and position achieved by any particle. After the comparison stage, the particles velocities are updated to make the particles converge to the best global and individual fitting. To fully emulate a swarm, the velocities are also regulated by a Momentum parameter. The Momentum decreases with each iteration, simulating fatigue within the particles in a moment when they should be near the minimum value (KARIMI et al., 2012). An explanatory pseudocode containing the described numeric procedure is presented in Table 5.

Table 5 - Particle Swarm Optimization Pseudocode

Initialization

Set Initial Parameters: *Population Size, Number of Iterations, Initial Momentum, Velocity Actualization Parameters*

Generates the population with random positions and velocities

Generates best global and particular values and positions

Imports the experimental data for the error minimization and validation

Main Loop

While: the Number of Iterations < Maximum Iterations OR Error < Tolerance:

Error Minimization – Network Optimization

For - *Each Individual in the Population:*

Checks the fitting for the particle this instant

If - *The present fitting is smaller than the personal best* **Then:**

This vector becomes the personal best (pbest) position and value

End If

If - *The present fitting is smaller than the swarm's best* **Then:**

This vector becomes the global best (gbest) position and value

End If

Convergence Improvement

Updates the velocity according to the best values and social parameters

Decreases the swarm's momentum by a fixed value

End For

If - *The number of iterations is enough* **Then:**

Randomizes positions and velocities to reinitialized the swarm

End If

End For

Final Procedures

Tests the experimental data against the system output

During this study, the algorithms worked with a population of 10 particles and for 200 iterations. The social parameters (KENEDY & EBERHART, 2001) c_1 and c_2 responsible for the weighting in the velocities update were set to 2.00 and 2.10 respectively. The equation that updates the velocity is presented in Equation 18.

$$v_{k+1} = v_k + c_1 * rand() * (Best_{Personal} - x_k) + c_2 * rand() * (Best_{Global} - x_k) \quad \text{Equation 18}$$

Where, v_k is the particle's position, v_{k+1} is the next position, $rand()$ is a random number between 0 and 1, $Best_{Personal}$ is the particle's position with the best fitting, $Best_{Global}$ is the position that obtained the best fitting among all particle's and x_k is the particle's current position. The position update is presented in Equation 12.

$$x_{k+1} = x_k + M \cdot v_k \quad \text{Equation 19}$$

Where, x_{k+1} is the particle's next position and M the particle's momentum.

The momentum parameter was initially set to 0.99. However, after all the particle's velocities were updated, this parameter was decreased until it reached a value lower than 0.20, after this point the momentum was reinitialized to 0.99, and positions randomization were performed. This approach is necessary to relocate the swarm from a possible local minimal point.

After the optimization procedure ends, the confidence interval for each adjusted model is calculated. An approximate confidence region can be calculated using Equation 20 (HIMMELBLAU, 1970).

$$C.R. = s_{\hat{Y}_i}^2 \cdot F_{1-\alpha}[m, n-m] \quad \text{Equation 20}$$

Where $C.R.$ is the confidence region range, $s_{\hat{Y}_i}^2$ is the standard error for each parameter, $F_{1-\alpha}$ is the upper limit of the F-distribution, m is the number of parameters and n is the number of experimental data points.

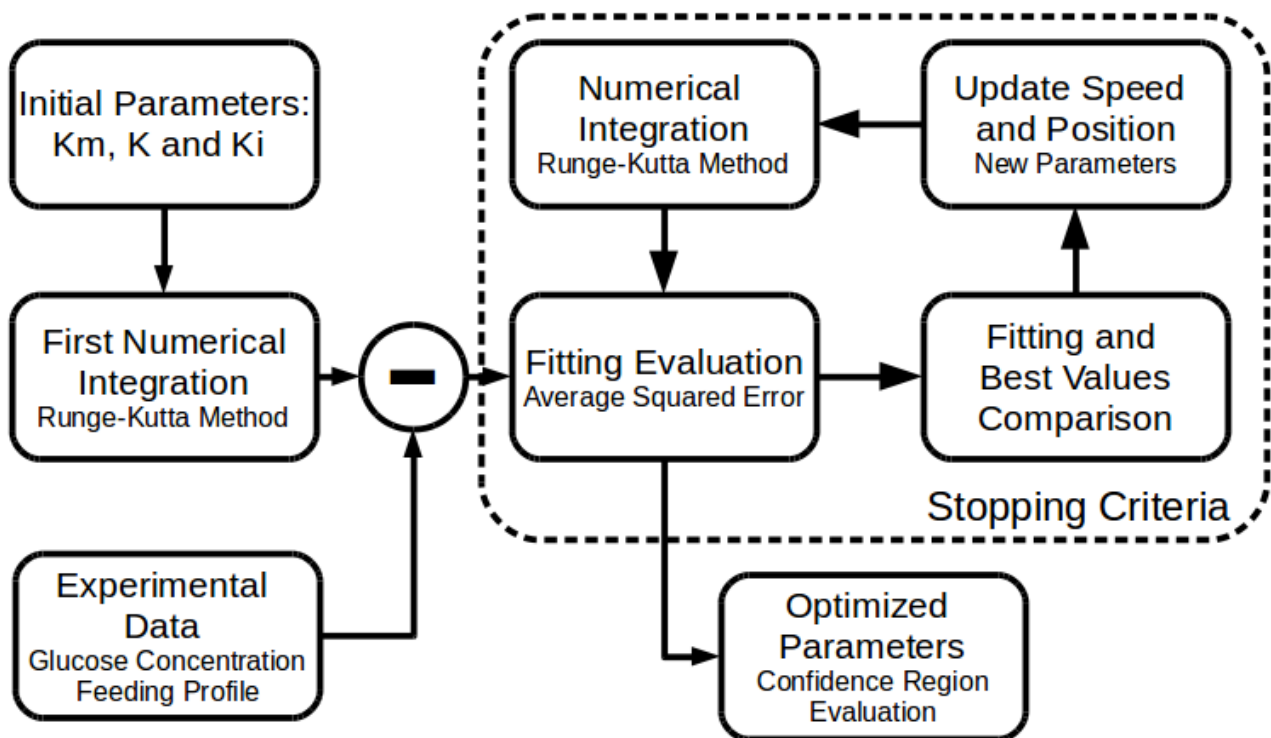
The contour for the sum of squares surface can be calculated according to Equation 21.

$$\phi = \phi_{min} \left\{ 1 + \frac{m}{(n-m)} \cdot F_{1-\alpha}[m, n-m] \right\} \quad \text{Equation 21}$$

Where ϕ is the squared error threshold for the region, if a parameters group has a squared error value higher than this value it is considered outside the confidence error and ϕ_{min} is the squared error for the optimized parameter (HIMMELBLAU, 1970).

The entire procedure follows the dynamic demonstrated in the Figure 5.

Figure 5 - Model Fitting Flowchart



(Source: author's collection)

3.6. FED-BATCH OPTIMIZATION

With the optimized models and its optimized parameters, the balance presented in item 3.5 was used to optimize the feeding strategy. The mass flow were subjected to an optimization method, where the profiles, both for substrate and enzymatic complex, changed at each iteration until an optimum bagasse and enzymatic complex addition is achieved.

The sequential approach and PSO algorithm, described in the previous item, were used to solve the optimal control problem. Therefore, the input flow had to be parameterized. Vectors with equal amount of points for bagasse and enzyme addition were created. The first value is the initial compound addition, and the other points are additions throughout the process.

For each evaluated feeding profiles, an integration of the fed-batch product balance is realized. The performance of the simulated feeding profile was evaluated by converting the final carbohydrate concentration into potential ethanol, via theoretical maximum stoichiometric coefficient, and subtracting from the revenue of selling this product the cost

of the enzymatic complex and electrical power necessary to agitate the reactor. This value is divided by the total mass of bagasse added in the process in order to generate a revenue related to the added mass (US\$.kg_{Bagasse}⁻¹). Hence the objective function becomes:

$$P\left(\frac{US \$}{kg_{bagasse}}\right) = \frac{m_{Ethanol} \cdot P_{Ethanol} - m_{Enzyme} \cdot P_{Enzyme} - P_{Power} \int_{t_0}^{t_f} P_{Agitation}}{m_{Bagasse}} \quad \text{Equation 22}$$

Where P is the Performance Index (PI) generated by the process, m_{Ethanol} is the glucose concentration converted to potential Ethanol, P_{ethanol} is the Ethanol selling price, m_{Enzyme} is the accumulated enzyme mass, P_{enzyme} is the Enzymatic Complex price, P_{power} is the electric energy price, and P_{Stirring} is the power necessary to agitate the reactor.

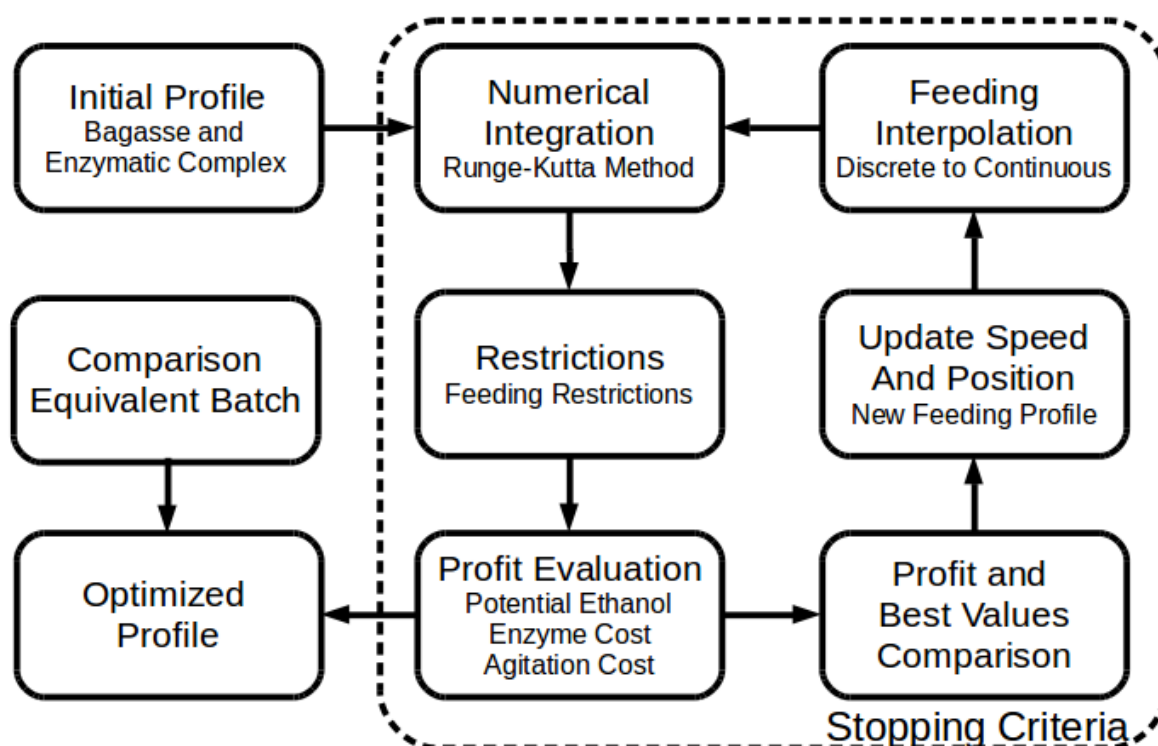
The price for ethanol was 1.50 US\$.kg⁻¹ (FURLAN et al. 2012), the evaluated cost of the accumulated enzymatic complex mass was 1.20 US\$.kg⁻¹ (FURLAN et al., 2012) and the electrical power cost was 59.00 US\$.Mwh⁻¹ (DIAS 2011). The solids fraction in the feeding flow was 0.40. The total times of fed-batch utilized in the optimization were; 360, 240, 144, 120, 96 and 48 h and feeding points were realized once an hour. The simulated reactor initial volume was 10 m³ and throughout the simulations no final reactor volume was applied.

A representation of how the optimization works is presented in Figure 6.

During the optimization, a series of restriction may be applied, to generate more feasible solutions. The profiles were subjected to maximum mass addition and maximum substrate concentrations at any given time.

After the optimization reached its stopping criteria, a batch process was simulated where the accumulated bagasse mass and accumulated enzymatic complex from the optimum profile were added in the beginning of the process. The batch process revenue was calculate following the methodology of the fed-batch process. This was performed in order to evaluate the differences between the batch and fed-batch processes.

Figure 6 - Feeding profile optimization



(Source: author's collection)

3.6.1. Stirring Power

A vital part of the process PI is the cost of energy in order to agitate the reactor. To estimate this cost a relation between the solids inside the reactor and the engine torque, and subsequent stirring power.

In order to achieve this relation, an empirical model was fitted between the stirring power acquired by monitoring system and the solids inside the reactor. However, solids concentration is not available experimentally. Thus, after the most accurate enzymatic velocity model is chosen, the model is adjusted to each batch experiment following the methodology presented in item 3.5. The balance of the solids output was used in the fitting of the empirical solids/stirring power model.

3.6.2. Hydrolysis Reactor Plant Equivalence

At the end of each optimization cycle, when the optimum profile was achieved, an extrapolation was performed to determine the reactor size necessary to operate a second generation ethanol production plant.

The fictitious plant operated alongside a standard ethanol plant, milling 500 t.h⁻¹ of

sugarcane. This generates, approximately, 132 t.h⁻¹ of bagasse, 20% of this bagasse was assumed to be used to produce second generation ethanol. Thus, the 2G plant must be able to process 26.4 t_{bagasse}.h⁻¹. To estimate the necessary reactor volume, or the volume sum of parallel reactors, the total processed bagasse was divided by the reactor final volume and process total time. This calculation is shown in Equation 23.

$$H.C. \cdot \left(\frac{t_{bagasse}}{h \cdot m^3} \right) = \frac{m_{Accumulated\ Bagasse}}{t_f \cdot V_f} \quad \text{Equation 23}$$

Where H.C. is the hydrolysis capacity of the process, $m_{Accumulated\ Bagasse}$ is the total accumulated bagasse throughout the process, t_f is the process total time and V_f is the process volume at the final time.

This value was then multiplied by the necessary productivity (26.4 t_{bagasse}.h⁻¹) resulting in the volume necessary to process at this rate.

3.7. NEURAL NETWORK OPTIMIZATION

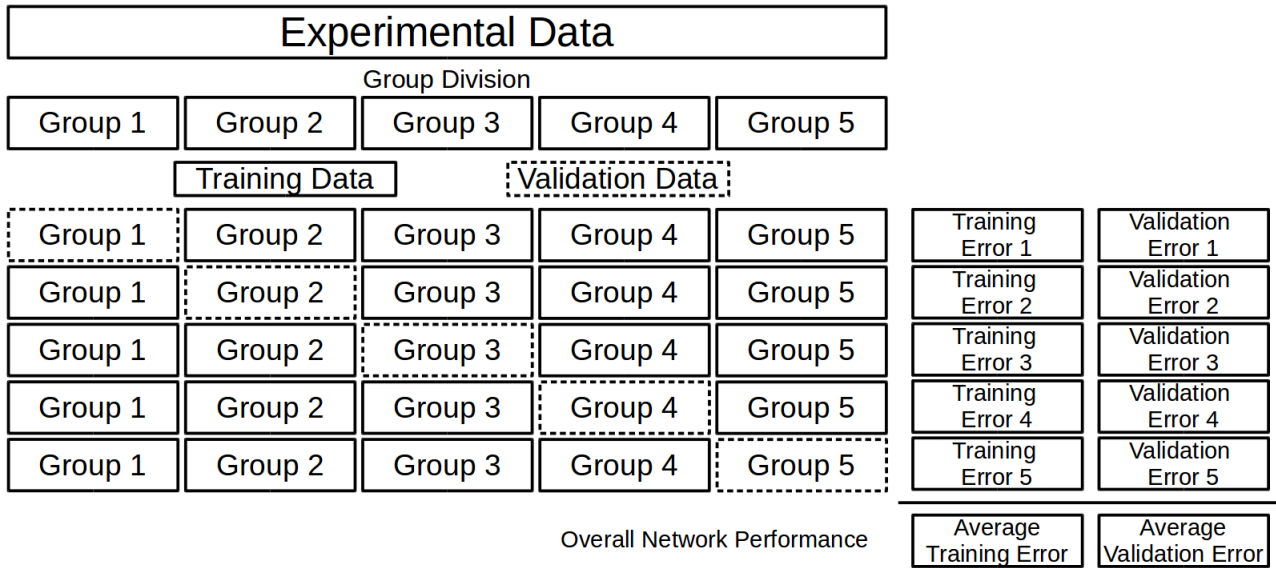
Neural Network (NN) models were used to translate the data from dynamometer and conductivity/capacitive probe to glucose concentration. The NN models were implemented in software Matlab 2012 using the Neural Network Toolbox.

The NN inputs were originated in the data provided by the instrumentation and the reactor state during the high volume batch and fed-batch hydrolysis and were: stirring power per reactor litter, conductivity, capacitance, accumulated substrate feeding and reactor volume; and the network output was the glucose concentration from the chromatography analysis. However, there were too few glucose experimental data points to train the NN correctly. To improve the network inference, the best kinetic model was adjusted for each experiment and the model predicted values were used in the network optimization.

Cross validation approach was used to avoid overfitting issues (NELLES, 2001). The sample universe was first randomized. The samples were then divided in 5 sets. To evaluate an architecture 4 sets were used while training the network (the current training group) and the unused set was used to validate (the validation group) the current training. This approach was repeated until all the sets were used as validation set. The average of the standard error of training and the average of the standard error of validation were used to evaluate the architecture performance. A graphical representation of this procedure is

presented in Figure 7.

Figure 7 – Cross Validation Procedure



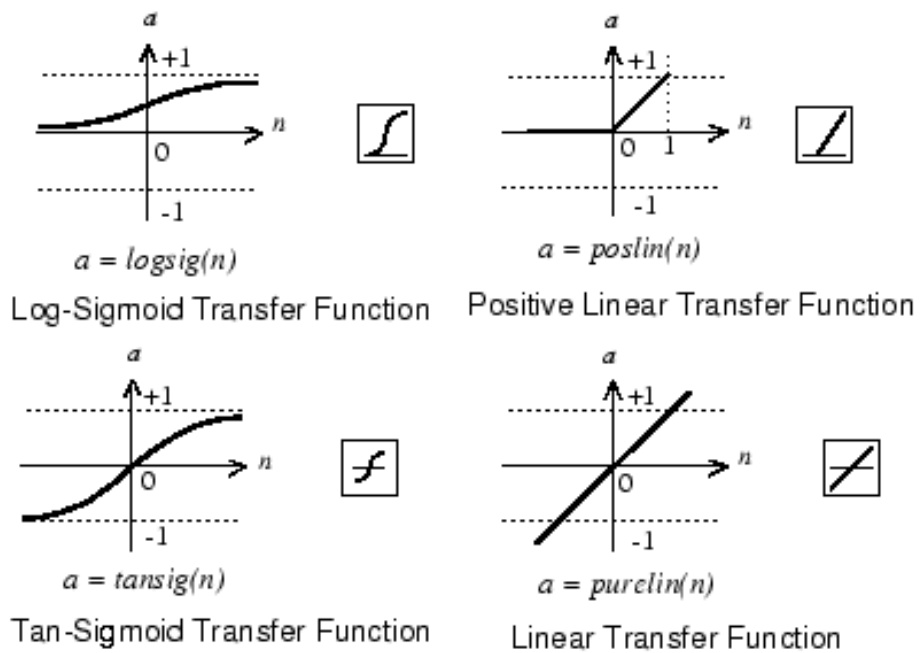
(Source: author’s collection)

The architectures taken into account were multilayer perceptrons with one hidden layer, the numbers of neurons in the hidden layer were 1, through 15. And the evaluated transfer functions for the hidden layer and the sum layer are displayed in Figure 8. Each transfer function was evaluated both for the hidden layer and the sum layer.

The NN optimum architecture is achieved when the average standard error from the validation departs from the linear tendency of accompanying the average standard error from the training. When this happens, a possible interpretation is that the complexity of the networks has become larger than the necessary for the system. The networks starts to contemplate, in the pattern recognition, the noise from the samples disrupting the network inference (overfitting).

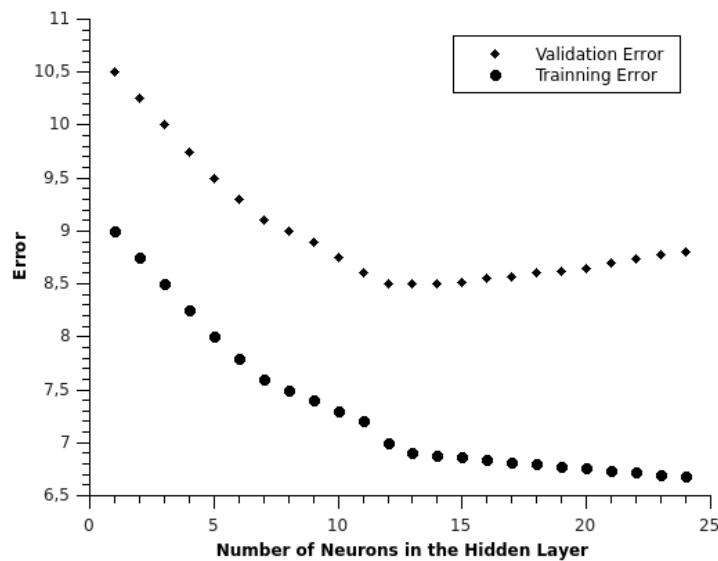
Therefore, the optimum architecture is when the errors are closely related (NELLES, 2001). An example of the behavior is presented in Figure 9. In the presented example, the point in which the validation error departs from the training error is at around 12 neurons in the hidden layer, thus demonstrating to be the optimum architecture for this hypothetical network.

Figure 8 - Evaluated transfer functions



(Source: author's collection, adapted from Matlab Neural Network Toolbox User's Guide)

Figure 9 - Training and Validation Data set Error



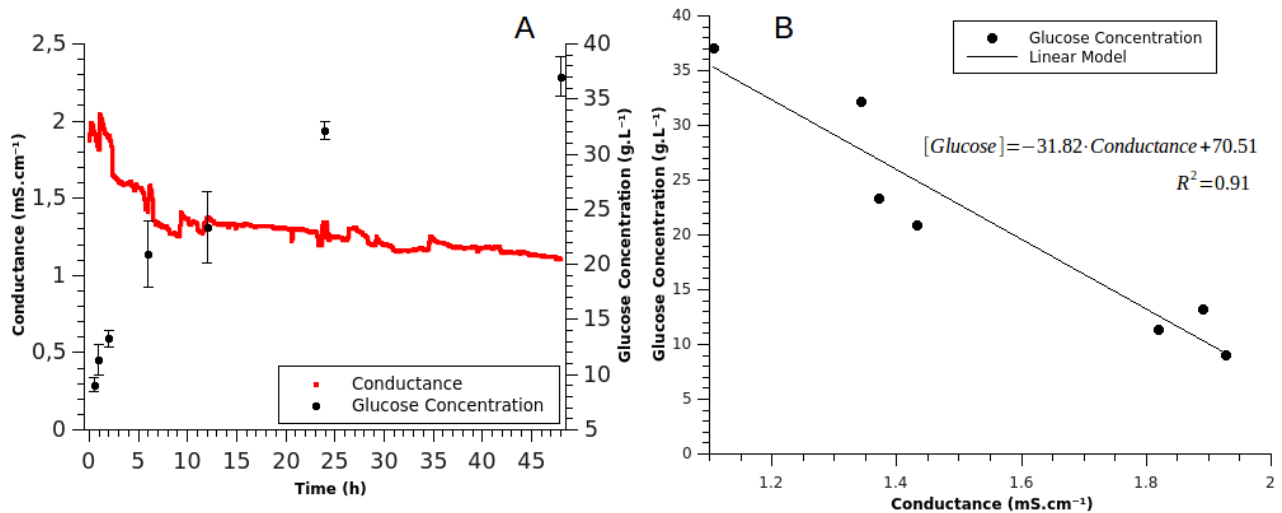
(Source: author's collection, adapted from NELLES, 2001)

4. RESULTS AND DISCUSSION

4.1. CONDUCTIVITY MONITORING

The experiments conducted in the 500 mL vessel provided the data presented in Figure 10.

Figure 10 - Conductance and glucose concentration during hydrolysis.



(Source: author's collection) (Where: Error bars are s.d. of triplicate measurements.)

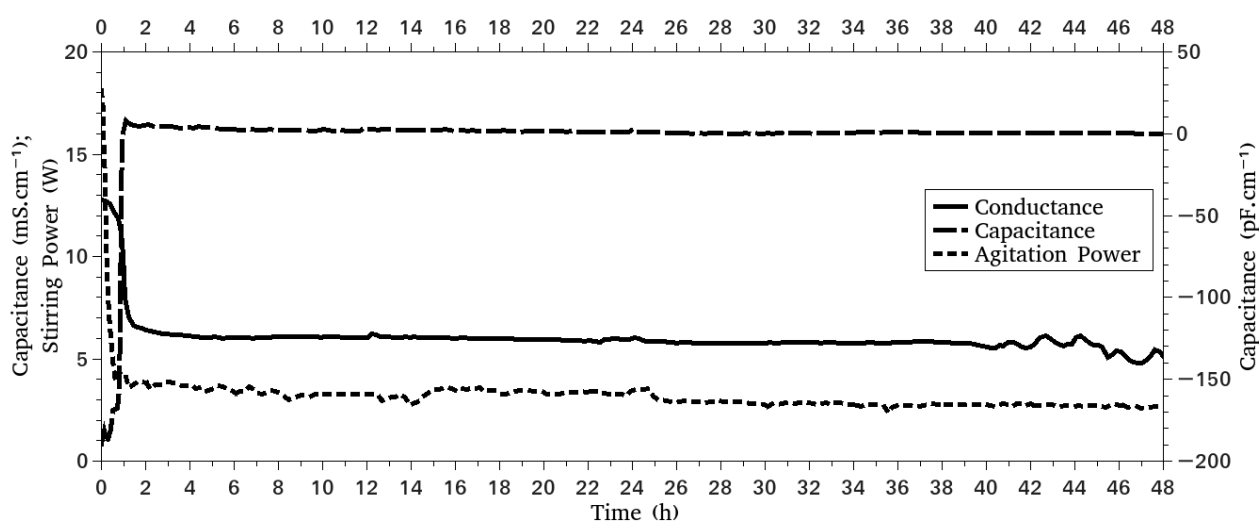
A linear negative correlation between conductance and glucose concentration in the medium supernatant was observed (see Figure 10 B), slope of -31.82, intercepting point of 70.51 and determination coefficient of 0.91. Thus, conductance may be a feasible option to follow real-time hydrolysis kinetics within the reactor. This motivates further studies using CCS to monitor the process.

Thus the conductance/capacitance probe was installed in the 3 L reactor to continue the studies.

4.2. FULL ARRAY INSTRUMENTATION

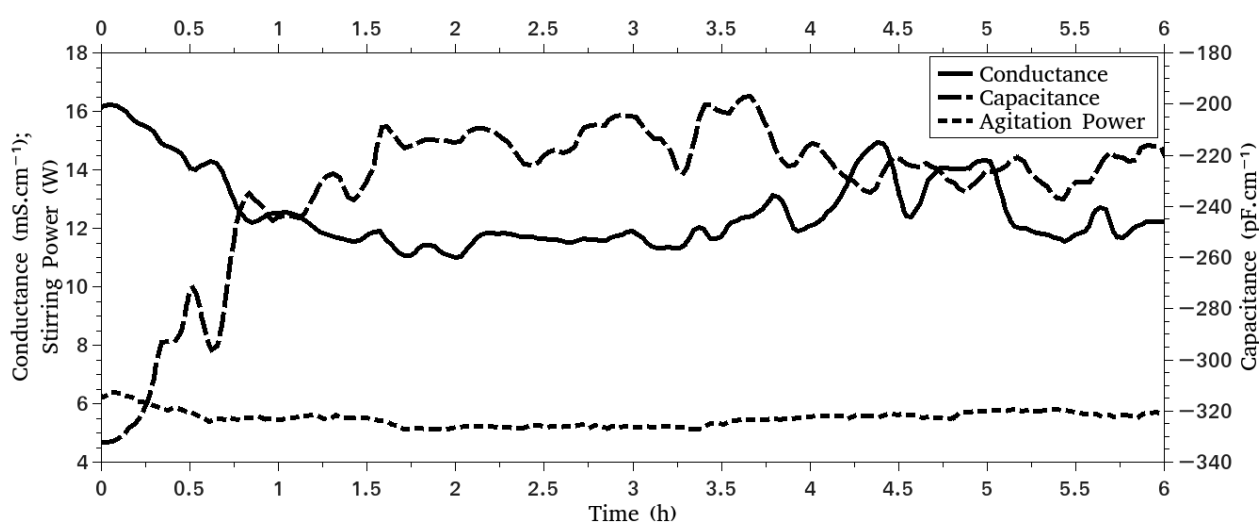
With the full array of sensors properly placed in the reactor, two experiments were conducted for each hydrolysis policy. The instrumentation data for agitation power, capacitance and conductance during the batch experiments are presented in Figure 11. Figure 12 presents the same instrumentation data for the fed-batch experiments.

Figure 11 - Full Array Monitoring During Batch Experiments



(Source: author's collection)

Figure 12 - Full Array Monitoring During Fed-batch Experiments



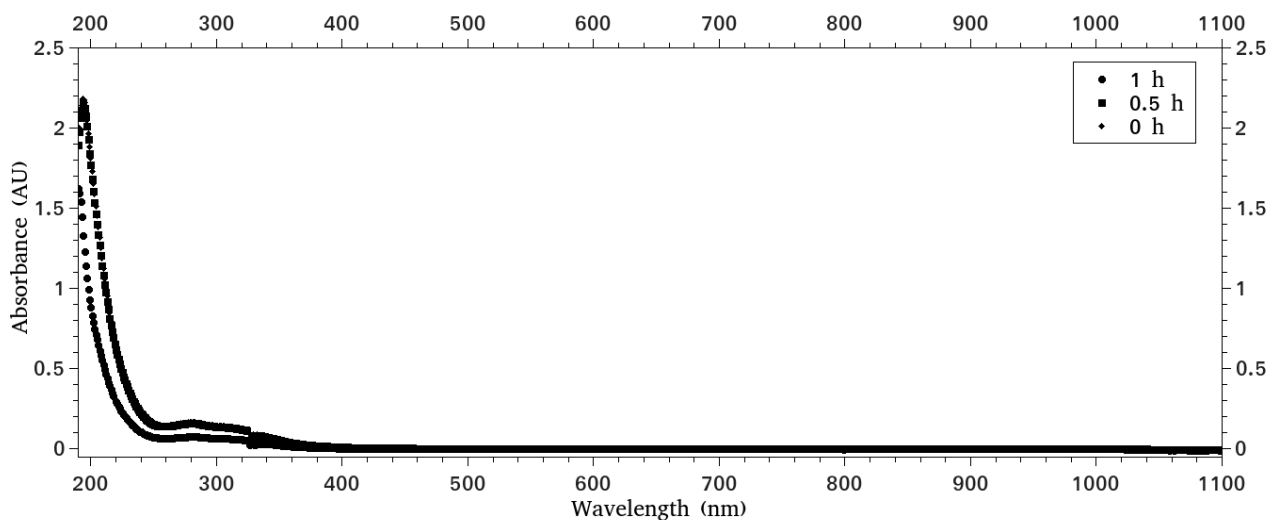
(Source: author's collection)

The capacitance/conductance probe and dynamometer were able to monitor the experiments throughout the process. However, the analytical line and supernatant UV/VIS scanning did not show a level of robustness necessary for the application.

The analytical line monitoring system initially was able to sample the reactive media, dilute the samples and communicate with the spectrophotometer. However, during long term experiments, the line had problems both in the software and hardware. At first, a problem occurred with the serial connections and analysis scheduling. After the solution of such problems, during the experiment the decrease in size of suspended solids particles

generated a cake on the filter membrane, which introduced a pressure drop that the used pump was not able to overcome, disabling the analytical line. Nevertheless, examples of sample scans in time periods where the analytical line was operating are presented in Figure 13, for the fed-batch experiments.

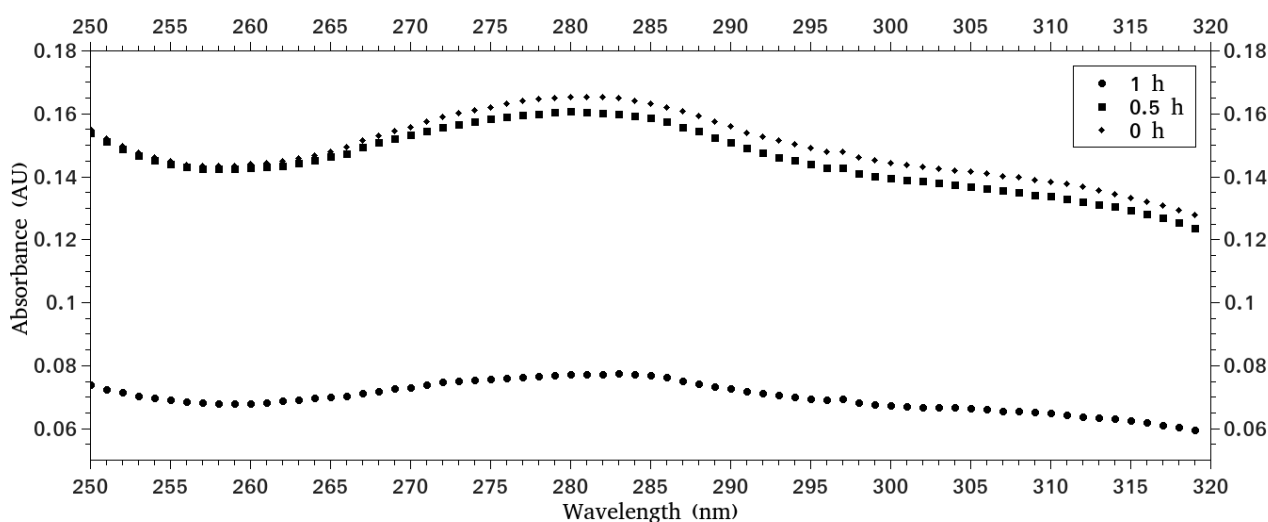
Figure 13 – Supernatant Scans During Fed-batch Experiments



(Source: author's collection)

The data curves overlapping hinders a better analysis, thus Figure 14 presents an amplification of the range between 220 and 400 nm.

Figure 14 – Supernatant Scans from 250 to 320 nm



(Source: author's collection)

A peak is present around the region of 283 nm. This peak may be correlated with the amount of lignin in the solution, since the same region is used in order to estimate this

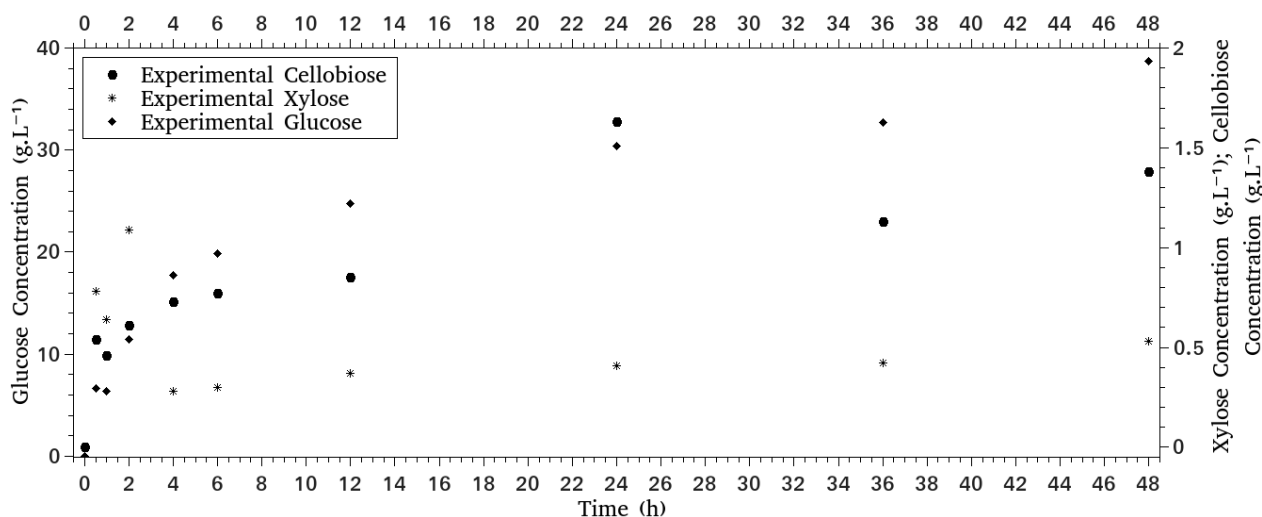
compound concentration in lignocellulosic materials (NREL, 2008; GOUVEIA et al., 2009; KLINE et al., 2010). Another important characteristic of the data-set is that the peak intensity rises with time. This may demonstrate that lignin is being released from the lignocellulosic matrix. Since lignin is an interferent in the process, binding irreversibly to the enzymatic complex (ARANTES & SADDLER, 2011), this instrumentation may be used in order to re-parametrize the enzymatic velocity model during the process, in order to assess the necessity of addition of enzymatic complex.

The robustness of this instrumentation setup was not reliable during the whole process, and the data generated from this analytical line was not used any further. Nonetheless this system may generate important data for the controller software. Thus, further studies will contemplate improvements in the analytical line in order to adequate it to the process.

4.3. BATCH AND FED-BATCH EXPERIMENTAL DATA

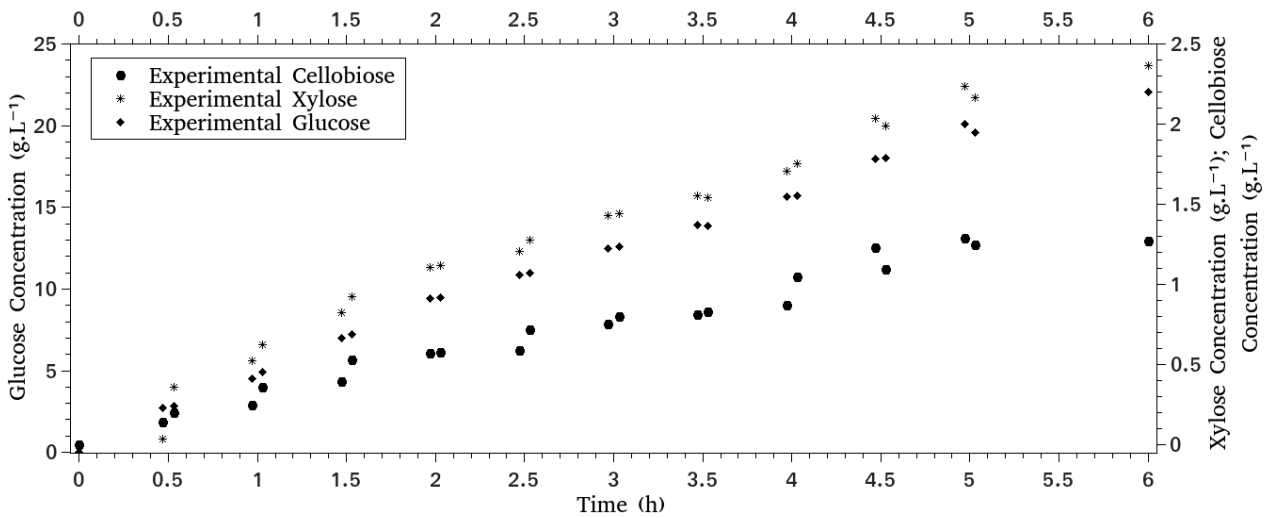
The measurements, generated from the HPLC, for the experiments conducted in the 5 L reactor, are presented in Figure 15 for the batch runs and Figure 16 for the fed-batch policy.

Figure 15 – Experimental Data for Batch Experiments



(Source: author's collection)

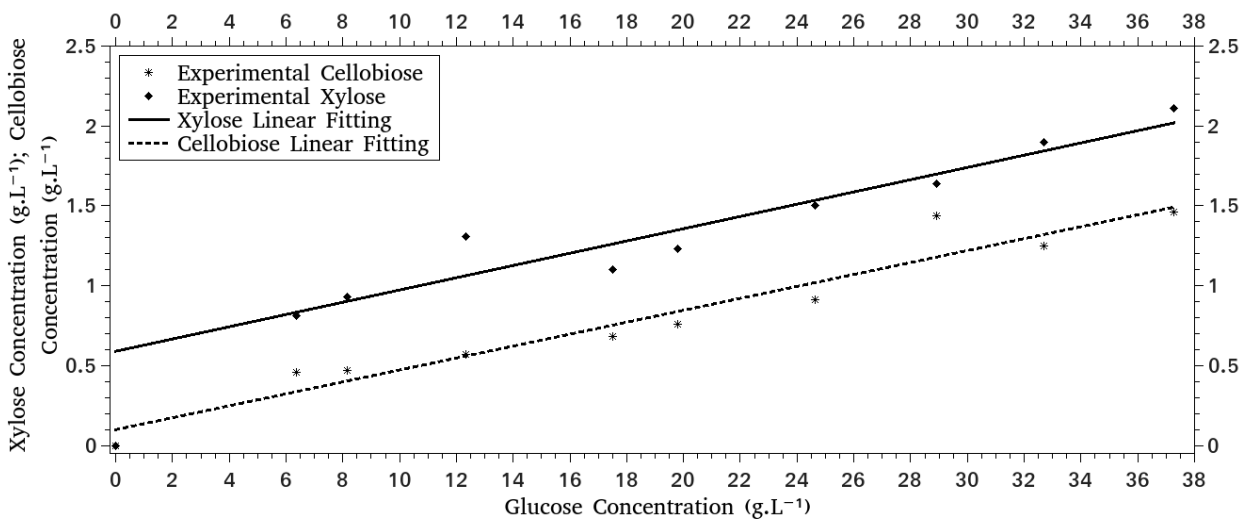
Figure 16 – Experimental Data for Fed-batch Experiments



(Source: author’s collection)

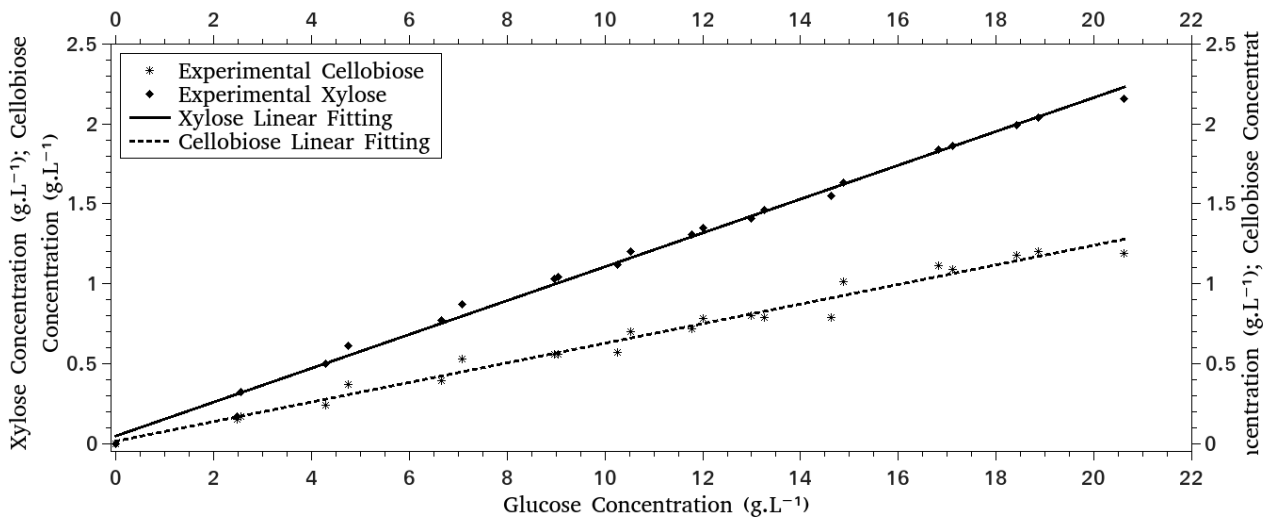
Since the concentrations of xylose and cellobiose are small, instead of fitting kinetic models for the production of these carbohydrates, the experimental data were used to adjust a pseudo-stoichiometric ratio between glucose and the xylose and cellobiose concentrations. Glucose concentration and the concentrations of xylose and cellobiose at the same time were correlated, as it can be seen in Figure 17, for the batch experiments, and in Figure 18, for the fed-batch experiments.

Figure 17 – Batch Experiments Co-products Linear Fitting



(Source: author’s collection)

Figure 18 – Batch Experiments Co-products Linear Fitting



(Source: author’s collection)

The parameters for each linear fitting is presented in Table 6.

Table 6 – Co-products Linear Fitting

Policy	Compound	Slope	Intercepting Point	Determination Coefficient
Batch Experiment	Xylose	0.0384	0.5894	0.9225
	Cellobiose	0.0350	0.1595	0.9140
Fed-batch Experiment	Xylose	0.1050	0.0590	0.9940
	Cellobiose	0.0608	0.0214	0.9732

This is an empirical approach, since the ratio between these products is actually dictated by their rates of formation – which depend on the enzymatic kinetics of a complex system of reactions, on mass transfer resistances, on the deviation from ideal mixing in the bioreactor, among other phenomena. This is the reason for obtaining different slopes in the correlations for batch and fed-batch operation.

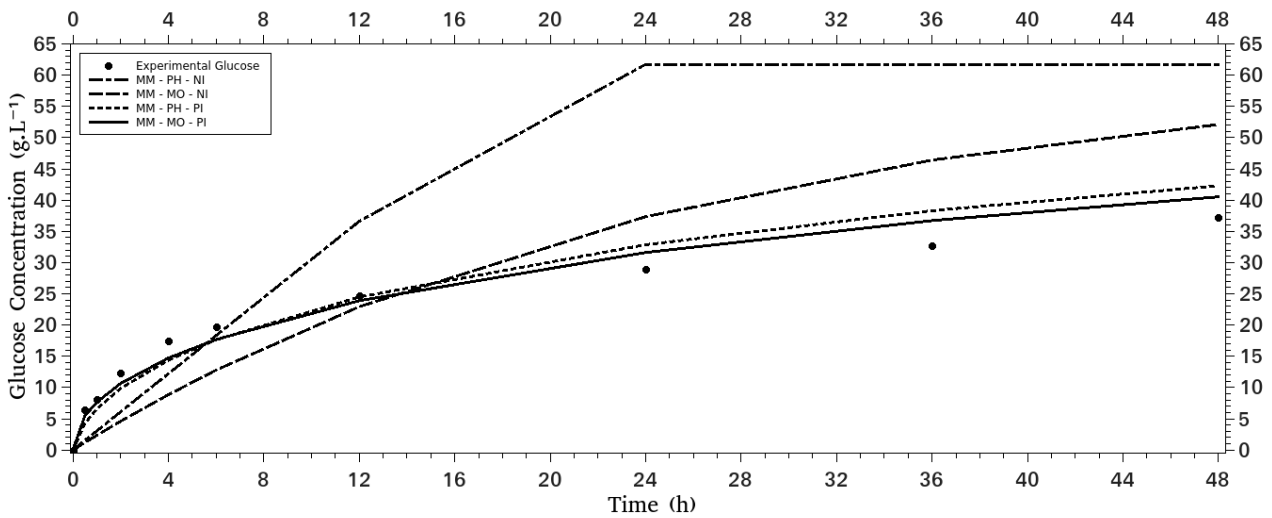
However, since the focus of this work is on implementing and testing automation algorithms, and taking into account that the linear correlations adhered very well to the experimental data, this simplification was adopted – implying that only one kinetic model had to be fitted, describing the formation of glucose.

4.4. PARAMETERS FITTING

The models presented in Item 2.4.1. were adjusted to the experimental data

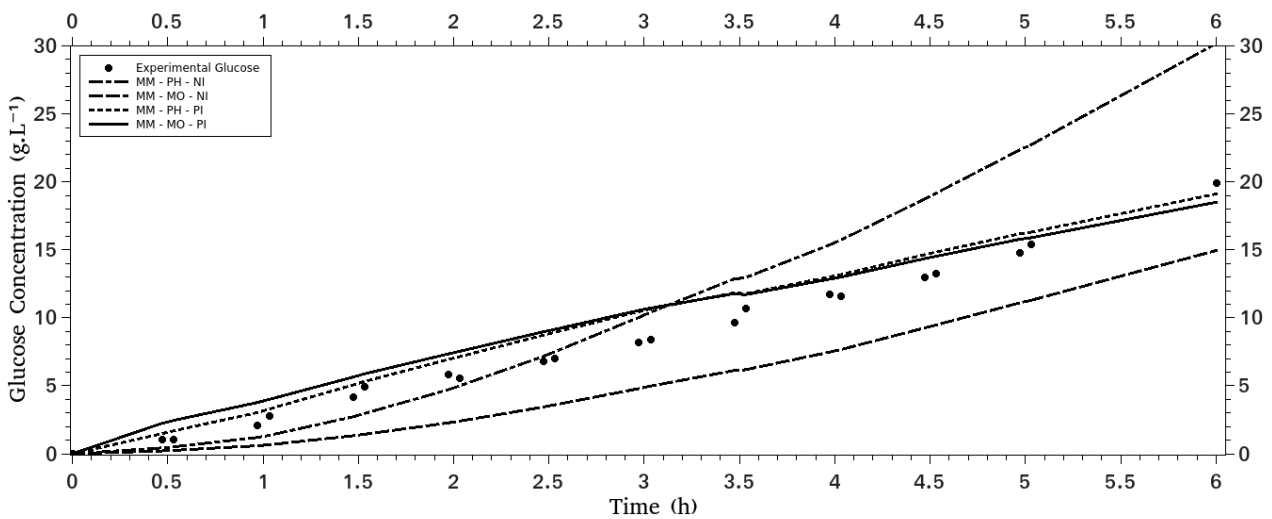
presented in Item 4.3. The models and experimental data are presented in Figure 19 for the batch experiments and Figure 20 for the fed-batch experiments.

Figure 19 - Model fitting for Batch Experiments



(Source: author's collection) (Where: MM – Michaelis-Mentem; PH – Pseudo Homogeneous; MO – Modified; NI – Non Inhibit; PI – Product Inhibited)

Figure 20 – Model Fitting for Fed-batch Experiments



(Source: author's collection) (Where: MM – Michaelis-Mentem; PH – Pseudo Homogeneous; MO – Modified; NI – Non Inhibit; PI – Product Inhibited)

The parameters, from the models are presented in Table 7.

The analysis of the Figures and Table show that the models containing product inhibition were able to fit the data in a satisfactory manner. The models without product inhibition did not present an adequate adherence. However, a lack of fitting is observed in

the final stages of the hydrolysis, especially for the long term batch policies. This demonstrates that another inhibition phenomenon is occurring within the process.

To improve modeling at the final stages of the hydrolysis it is necessary to evaluate other causes for inhibition or deactivation, such as thermal denaturation, or the addition of other compounds into the balance that may interfere in the system dynamics.

Table 7 – Models Parameters with 95% confidence intervals

Model	Parameters			Average Error
	Km (g.L ⁻¹)	K (min ⁻¹)	Ki (g.L ⁻¹)	
Pseudo-Homogeneous Michaelis-Mentem Non Inhibited	0.084±0.06	0.146±0.12	-	13.409
Pseudo-Homogeneous Michaelis-Mentem Product Inhibited	3.387±1.49	0.805±0.53	0.129±0.06	4.138
Modified Michaelis-Mentem Non Inhibited	29.597±24.42	0.055±0.03	-	13.846
Modified Michaelis-Mentem Product Inhibited	2.881±0.69	0.666±0.32	0.110±0.04	3.542

From the tested models, the one that presented the smallest average error, as well as the smallest confidence intervals was the modified Michaelis-Mentem model with product inhibition. Table 8 presents their correlation matrix.

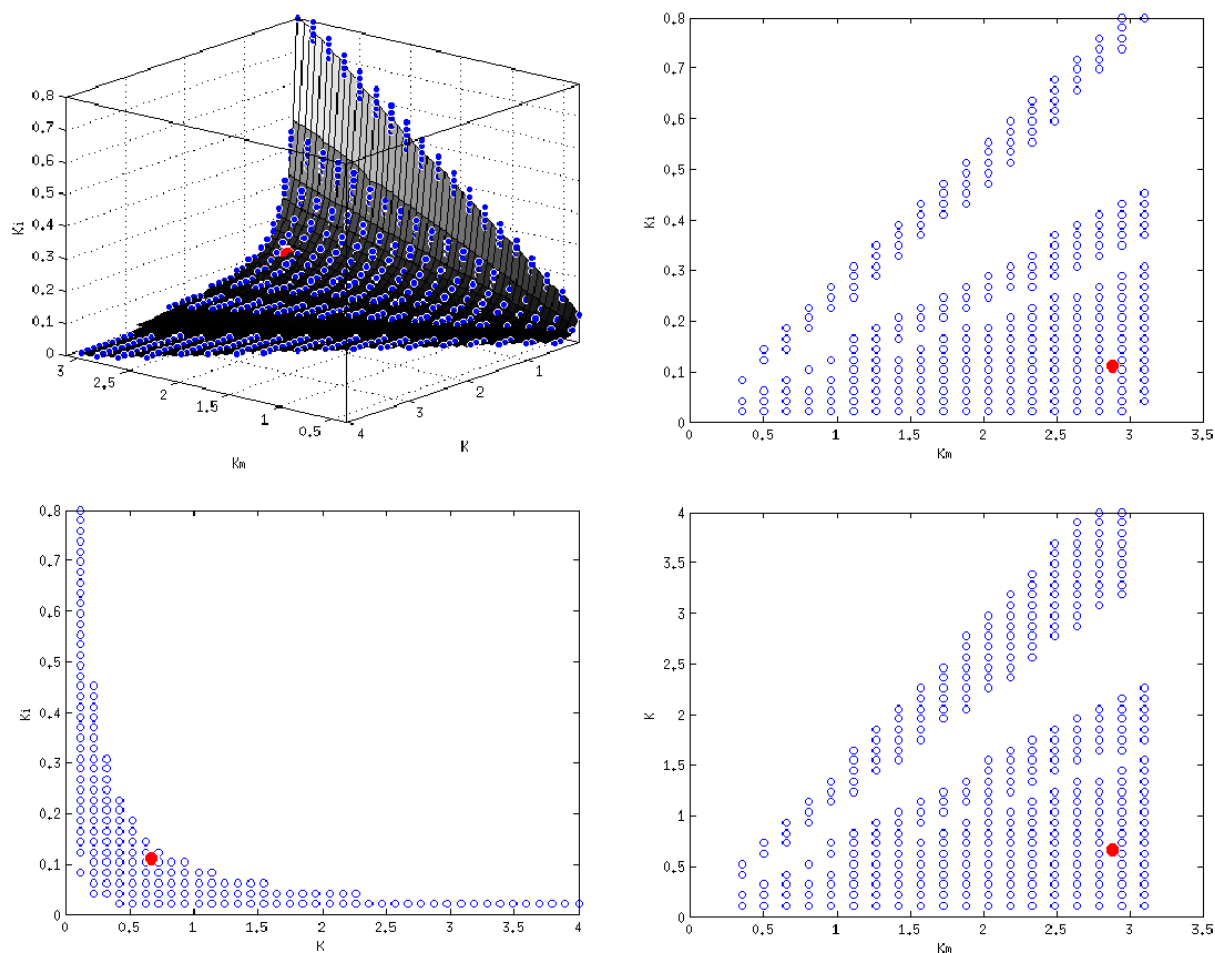
Table 8 – Correlation Table for the Modified MM Model with Product Inhibition

Parameter	Km	K	Ki
Km	1.00	0.62	-0.45
K	0.62	1.00	-0.94
Ki	-0.45	-0.94	1.00

The relative high correlation between the parameters demonstrates that the model, even though with very important simplifications, is fitting the data with very acceptable accuracy.

Figure 21 that demonstrates the confidence region at 95% confidence.

Figure 21 – Confidence Region for the Modified MM Model with Product Inhibition.



(Source: author's collection) (Where: Blue dots are data points inside the 95% confidence region and red dot optimum parameters)

The confidence interval topology indicates, once again, that the parameters are highly correlated, and so it is expected that the current state of the reactor will have important effect on the results of the online re-parametrization of the model. This behavior further demonstrates the necessity of software for online re-parametrization of the model, in order to predict the kinetics of the reaction more accurately.

Carvalho et al. (2013) fitted the same kinetic models, but their substrate was steam exploded delignified (4% NaOH) bagasse, and the enzyme was Accellerase 1500[®]. Their experiments were carried on with 6.54% of solids (w.w⁻¹), 5.7 FPU.g⁻¹ Pretreated Bagasse and in batch runs only. The modified MM model with product inhibition was also the most suitable kinetic model, and their adjusted parameters were: K: 0.0033±7.10⁻⁴ min⁻¹, Km: 22.06±10.28 g.L⁻¹, Ki: 7.61±0.87 g.L⁻¹. Furthermore, a high correlation among the

parameters was also found. A nonlinear confidence region with a topology very similar to the one obtained here was observed as well.

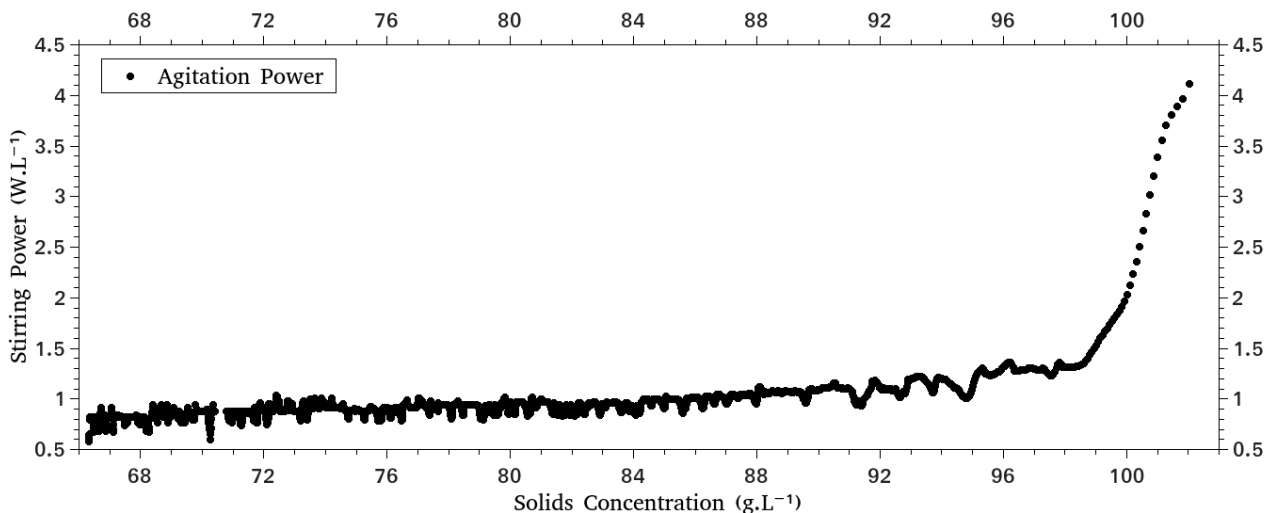
Although this model is based on very important simplifications of the problem, the comparison between the two optimized sets of parameters may suggest some conjectures: Carvalho et al. (2013) used Accelerase 1500[®], thus a lower value for K and a higher value for Km (when compared to the ones obtained in this work, using Cellic Ctec 2[®]) is not an unexpected result, since Cellic Ctec 2[®] is a more recent commercial cocktail. On the other hand, a higher Ki value in Carvalho et al. (2013) may be attributed to their bagasse pretreatment, capable of diminishing lignin content (that provided a substrate with only 5.37 % w.w⁻¹ of lignin, while in this work the lignin content was approximately 25% w.w.⁻¹).

The modified Michaelis-Mentem model with product inhibition, with the optimized parameters, was used in the following items to predict values at times not contemplated by experimental analysis or to predict variables where experimental data were not available.

4.5. STIRRING POWER/SOLIDS RELATION

With the predicted values from the adjusted models to the experimental batch policy data, the solids concentration and stirring power scatter is presented in Figure 22.

Figure 22 – Stirring Power/Solids Concentration Scatter Plot

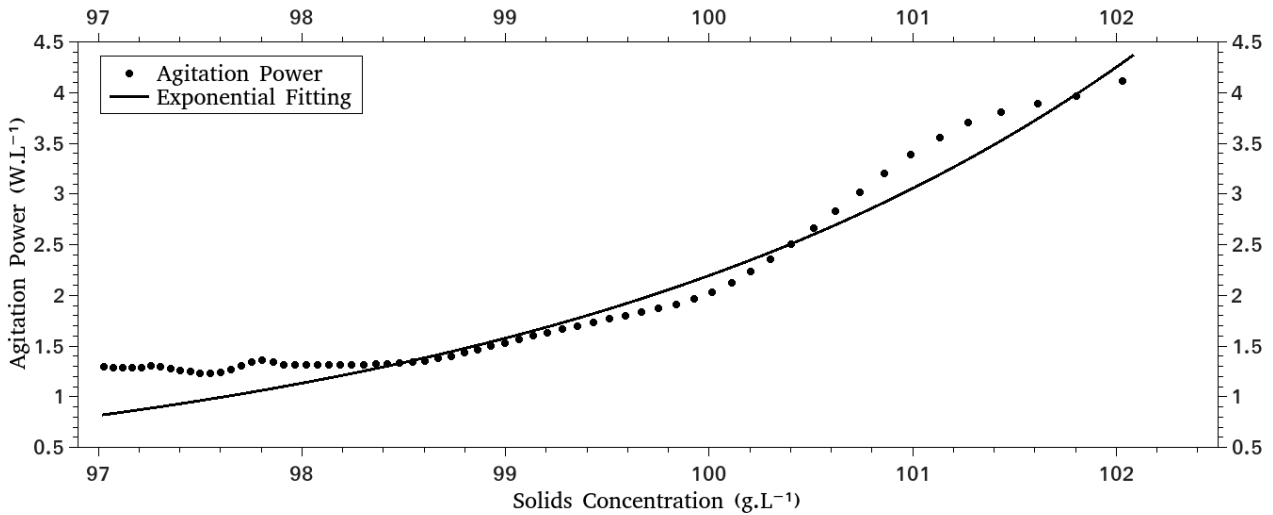


(Source: author's collection)

The figure presents two behaviors, with a threshold around 97 g.L⁻¹. Therefore, the fitting of only one empirical model to the entire range of concentrations may not generate

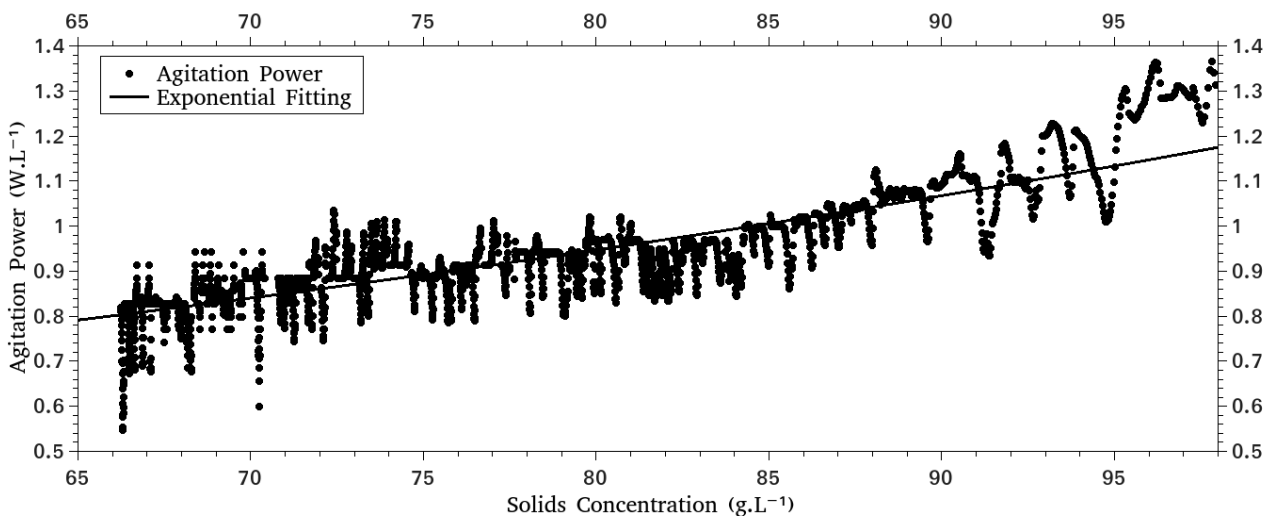
the necessary adherence. Thus, the profile was divided into two regions, one before and one after the 97 g.L⁻¹ solids marker. Both regions were subjected to an exponential fitting, the Figure 23, and Figure 24.

Figure 23 – Solids Above 97 g.L⁻¹ Region Exponential Fitting



(Source: author's collection)

Figure 24 – Solids Below 97 g.L⁻¹ Region Exponential Fitting



(Source: author's collection)

The adjusted models are presented in Table 9.

The analysis of both the figures and table presents that the fitting of the region with higher solids concentration is more accurate. However, this fitting improvement is achieved since the data in this region is more sparse and with less inherent noise.

Nevertheless, the models were employed in order to predict the power necessary to

agitate a vessel in a given solids concentration.

Table 9 – Stirring Power Fitting Models

Region	Exponential Model	Determination Coefficient
Bellow 97 g.L ⁻¹	$Agitation\ Power = 0.36 \cdot e^{0.01 \cdot [Solids]}$	0.72
Above 97 g.L ⁻¹	$Agitation\ Power = 9.81 \cdot 10^{-15} \cdot e^{0.33 \cdot [Solids]}$	0.97

These models were employed in predict the power necessary to agitate the vessel in a given concentration of solids. However, further studies must contemplate the utilization of more appropriate models, as well as include further assays to elucidate the relation among agitation power, solids concentration and reactor volume.

4.6. FEEDING PROFILE OPTIMIZATION

The feeding profile optimization, as describe in Item 3.6. was done using as the model optimized in Item 4.4 to predict reactions rates, and both models presented in Item 4.5 to estimate the energy demand for stirring the vessel.

The optimizer was applied without any restrictions on the optimization/operational variables. A summary of the optimizations is presented in Table 10.

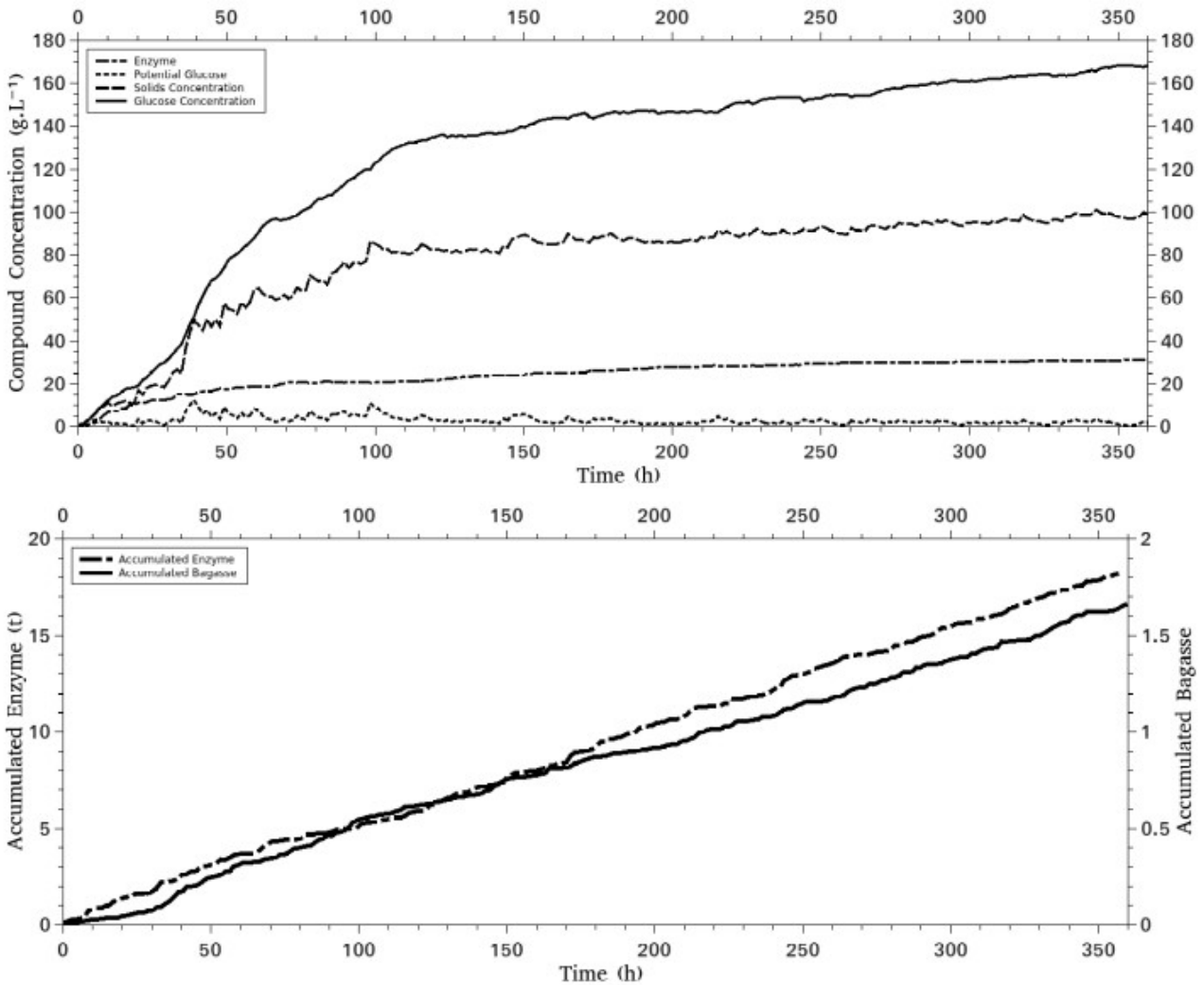
Table 10 – Unrestricted Feeding Policy

Total Time (h)	Final Volume (m ³)	Total Solids (t)	Total Enzyme (t)	Total FPU (FPU. g _{Bagasse} ⁻¹)	Fed-batch PI (US\$. t _{Bagasse} ⁻¹)	Batch PI (US\$. t _{Bagasse} ⁻¹)	Final Glucose (g.L ⁻¹)	Plant Volume (m ³)
48	17.55	3.56	0.16	137.98	359.46	< -1.10 ⁻⁶	122.57	6246.9
96	20.01	4.75	0.25	156.57	361.17	< -1.10 ⁻⁶	143.64	10674.0
120	26.86	7.13	0.49	202.69	345.49	< -1.10 ⁻⁶	160.62	11932.3
144	30.95	8.42	0.63	219.07	335.83	< -1.10 ⁻⁶	164.62	13971.0
240	43.51	12.14	1.16	279.27	310.57	< -1.10 ⁻⁶	166.89	22701.6
360	58.95	16.57	1.82	322.22	278.11	< -1.10 ⁻⁶	168.35	33815.1

The analysis of Table 10 demonstrates that all fed-batch situations generated a positive PI at the end of the process, while their equivalent batch counterparts, did not. This is related to the fact that an equivalent batch would with a very high solids (bagasse) concentration, generating a high agitation cost. During the fed-batch process, the optimization tool naturally converges to smaller solids concentrations, to reduce energy necessities bellow the threshold between the two agitation power models, where electricity cost is lower. This behavior is presented in Figure 25, that shows the profiles of the

compounds in the reactor, as well as the accumulated feedings.

Figure 25 – Fed-batch Optimization for 360 h Process



(Source: author's collection)

To maintain solids concentration at low values, a large volume of reactor, or reactors, is necessary to process the stream of bagasse described in Item 3.6.2, especially in long term processes, when the amount of bagasse added to the reactor increases considerably.

The simulations show that there is a clear trade-off between PI and the final product concentration. This occurs because longer processes enables a longer interaction between substrate and enzyme, decreasing solids concentration, and allowing more solids to be added. Since the addition of solids also dilutes the reactor, more enzyme is added in order to sustain the reaction velocity. All this generates a higher productivity, with a higher product final concentration.

However, more solids generates the necessity for more enzymatic complex, making the process more expensive. This is also true for the agitation power. As the process time increases so does the energy necessary to agitate the vessel. This however is not true for the 48h process, where the PI and product concentration are lower than the other processes. This is explained by the fact that in a process as short as the 48h there is not enough time to convert the substrate into product, generating a costly process and with small product concentration.

This tradeoff is important since a possible alternative in the utilization of the hydrolyzed lignocellulosic biomass is stream integration (MACRELLI et al., 2012). This is the process of combining the sugar rich currents from the sugarcane mill and the hydrolysis reactor product. However, both streams must have similar concentrations, so that one will not dilute the other. Since the sugarcane juice carbohydrate concentration is around 180 g.L^{-1} (FURLAN et al., 2013), the hydrolyzed liquor must be concentrated through evaporation if glucose end concentrations are too far from this target. Evaporating the hydrolysis product increases the cost of the process (notice that this cost was not considered in the PI defined here). Thus, the PI of the 48h process may be diminished. On the other hand, the longer (and with smaller PI) process may need less energy to concentrate the liquor, possibly generating a more attractive situation.

It should be stressed that the approach used here for defining PI isolates the reactor from the rest of the process. The resulting solutions may actually be sub-optimal, but an algorithm for online optimal control most certainly will be working within this approach, when dealing with real case industrial applications. Of course, some concatenation with a plant-wide optimization is desirable. One way to improve the link between local and global optimization is improving the calculation of PI. For instance, energy costs for concentration of the reactor effluent may be correlated to the contents of glucose in this stream. These ideas will be left as a suggestion for future work.

Nevertheless, in the presented simulations, the amount of enzymatic complex used in the process is not feasible for a large scale process. Enzyme mass in relation to the substrate reaches values that would rule out this process. The batch processes used in the composition of the velocity models used $10 \text{ FPU.g}_{\text{Bagasse}}$, and the optimizations reached values 30 times higher than this. This may be related to the fact that the optimizer needs a small concentration of solids in order to achieve favorable PI situations. Thus, a large amount of enzyme is added in order to decrease solids rapidly.

To diminish this effect, the same optimization sequence was repeated. But now the cost of energy to agitate the reactor was not taken into consideration when calculating the process PI. The new simulation summary is presented in Table 11.

Table 11 – Unrestricted Feeding Policy Without Stirring Cost

Total Time (h)	Final Volume (m ³)	Total Solids (t)	Total Enzyme (t)	Total FPU (FPU. g _{Bagasse} ⁻¹)	Fed-batch PI (US\$. t _{Bagasse} ⁻¹)	Batch PI (US\$. t _{Bagasse} ⁻¹)	Final Glucose (g.L ⁻¹)	Plant Volume (m ³)
48	19.40	5.01	0.19	110.98	386.40	445.04	145.76	490.8
96	62.25	28.98	0.67	68.05	402.34	445.62	261.25	545.5
120	61.54	28.71	0.65	67.24	412.98	435.62	268.63	679.1
144	79.42	38.70	0.87	66.14	417.75	425.11	283.35	780.1
240	153.29	85.24	1.22	41.92	421.87	434.33	319.13	1139.4
360	220.23	124.16	1.84	43.41	431.20	415.59	330.87	1685.8

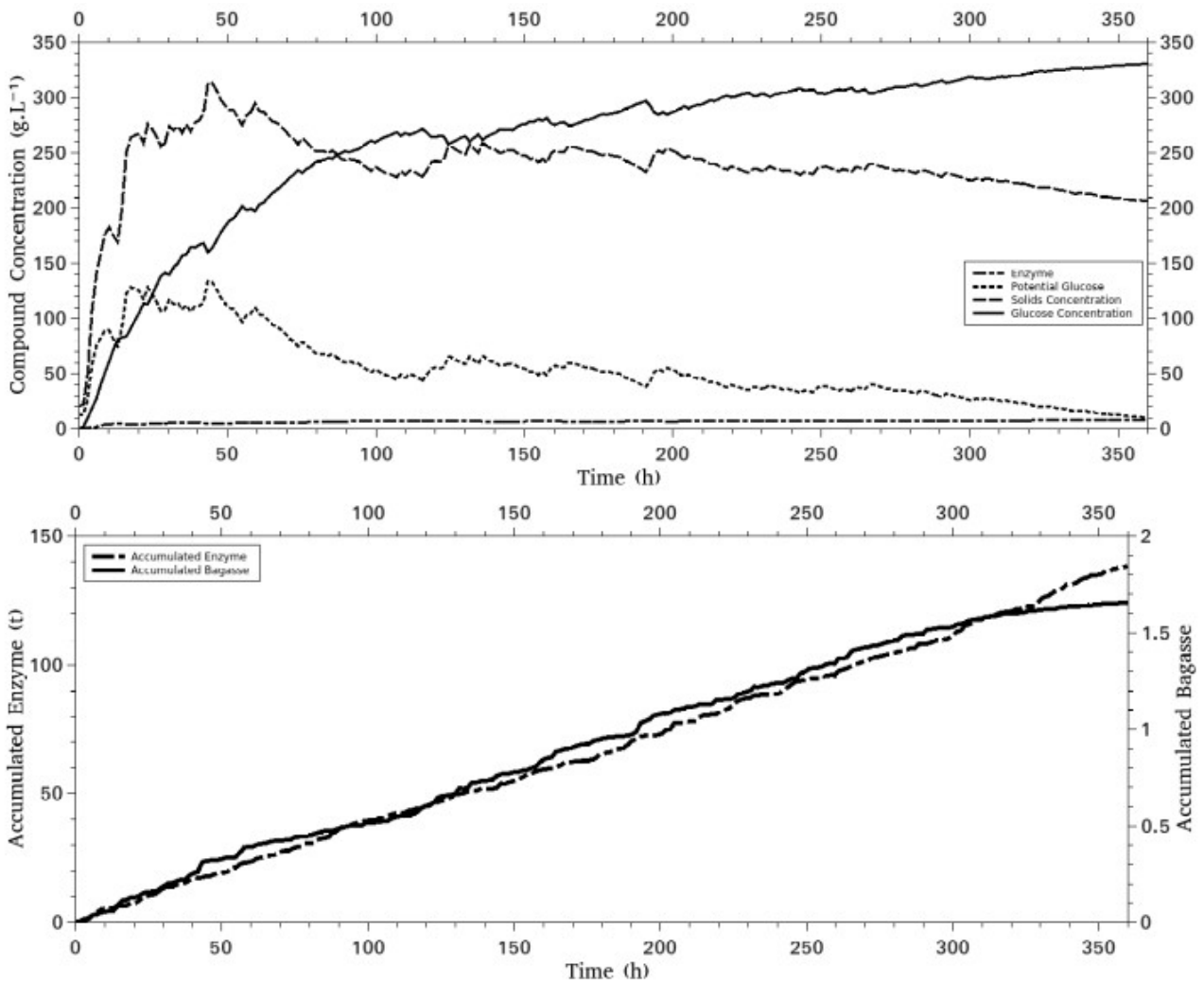
Disregarding the agitation power generated higher PI processes, since a part of cost was not accounted for, as well as diminished the necessity of enzymatic complex for each bagasse mass unit. This is because without the solids concentration limitation the substrate concentration does not need to be decreased as rapidly as in the last optimizations set to decrement agitation power. Therefore, less enzymatic complex needs to be added throughout the process. Higher solids concentration also generates higher end product concentration, even in short term operations.

Not having a cost limitation correlated with the solids concentrations also reduces the need for large operating volumes.

However, since there are no limitations on the stirring energy, solids concentration is let free to reach unfeasible regions. The profile presented in Figure 26 exemplifies this condition.

In this set of simulations solids concentration reached values higher than 30% w.v⁻¹. For the reactor design used in this work this is not a feasible situation. Solids deposition occurs at concentrations close to the agitation models threshold (97 g.L⁻¹).

Figure 26 – Fed-batch Optimization for 360 h Process Without Stirring Power



(Source: author's collection)

To overcome the solids concentration and enzyme loading problems, a final set of simulations were conducted. In these, the agitation power was accounted for in the same manner as in the first set of simulations. However, at this time a restriction on the enzyme addition was applied: the total accumulated enzyme could not surpass $50 \text{ FPU} \cdot \text{g}_{\text{Bagasse}}^{-1}$. This represents 5 times the amount used in the experiments assays and was considered a feasible value for large scale processes.

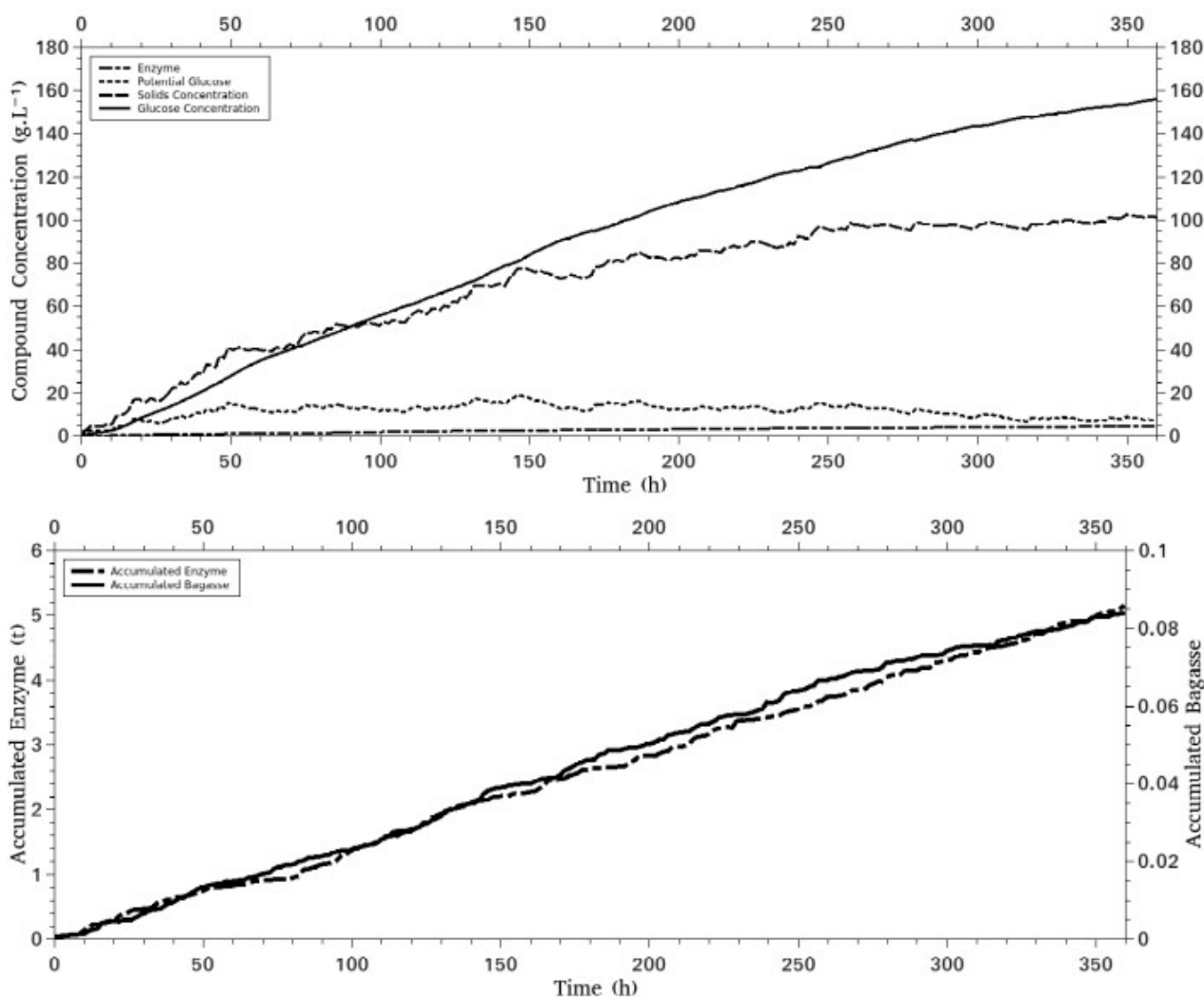
A summary of the optimizations is presented in Table 12.

Table 12 – Feeding Policy With Enzyme Addition Restriction

Total Time (h)	Final Volume (m ³)	Total Solids (t)	Total Enzyme (t)	Total FPU (FPU. g _{Bagasse} ⁻¹)	Fed-batch PI (US\$. t _{Bagasse} ⁻¹)	Batch PI (US\$. t _{Bagasse} ⁻¹)	Final Glucose (g.L ⁻¹)	Plant Volume (m ³)
48	11.27	0.75	0.01	47.58	297.11	404.67	29.13	19120.5
96	12.38	1.39	0.02	49.55	348.99	419.98	57.97	22540.1
120	13.30	1.93	0.03	49.53	353.97	-6.10 ⁻⁴	75.77	21887.1
144	13.85	2.28	0.03	43.68	354.79	< -1.10 ⁻⁶	86.64	23100.8
240	16.13	3.56	0.06	49.56	372.50	< -1.10 ⁻⁶	124.88	28714.8
360	18.64	5.03	0.09	49.74	352.97	< -1.10 ⁻⁶	156.05	35202.6

This strategy generated more feasible profiles, sustaining solids consistency and enzyme addition to an operational level. This is demonstrated in Figure 27.

Figure 27 – Fed-batch Optimization for 360 h Process With Feeding Restriction



(Source: author's collection)

The plant operational conditions for these simulations were similar to those without enzyme restriction, since the same behavior of maintaining low solids concentration was observed. The enzyme restriction would not greatly alter the reactor design, particularly when dealing with long term processes.

However, in these situations the final product concentration was lower than in the other data sets, especially in the short term operations. This is because the lower enzyme addition requires more time to hydrolyze the substrate. This solution would then require more energy for evaporation of the reactor outlet stream. In order to adequate this process to the 1G-2G carbohydrates stream combination either a longer operation is necessary or the final hydrolysis product must be concentrated.

Another possible solution is achieving higher solids concentrations without expanding a large amount of energy with agitation. To do that the reactor must be redesigned to work with higher solids concentrations.

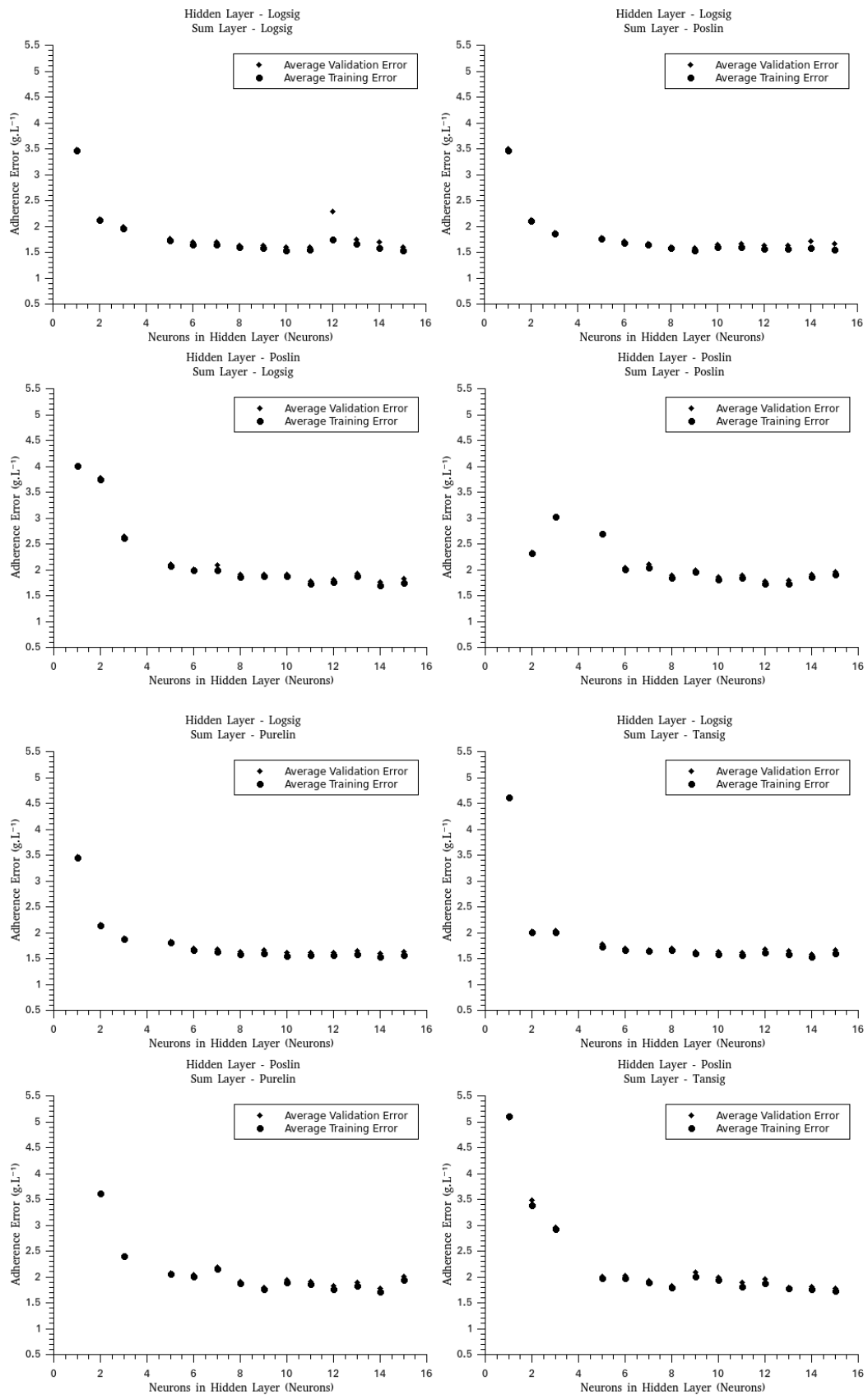
One design option is the utilization of a Continuous Tubular Screw Reactor (CTSR). This reactor uses a pressurized screw in order to move the bagasse from one end of the tube to the other. Meanwhile the solids are in contact with the enzymatic complex and hydrolysis occurs with lower energy consumption (TOMÁS et al., 1997).

The utilization of an alternative reactor design would promote a pre-hydrolysis at a solid consistency where the standard stirred tank would not be operational. After this first pre-hydrolysis, the more liquefied substrate can be directed to a standard reactor to finish the hydrolysis.

4.7. NEURAL NETWORK CALIBRATION

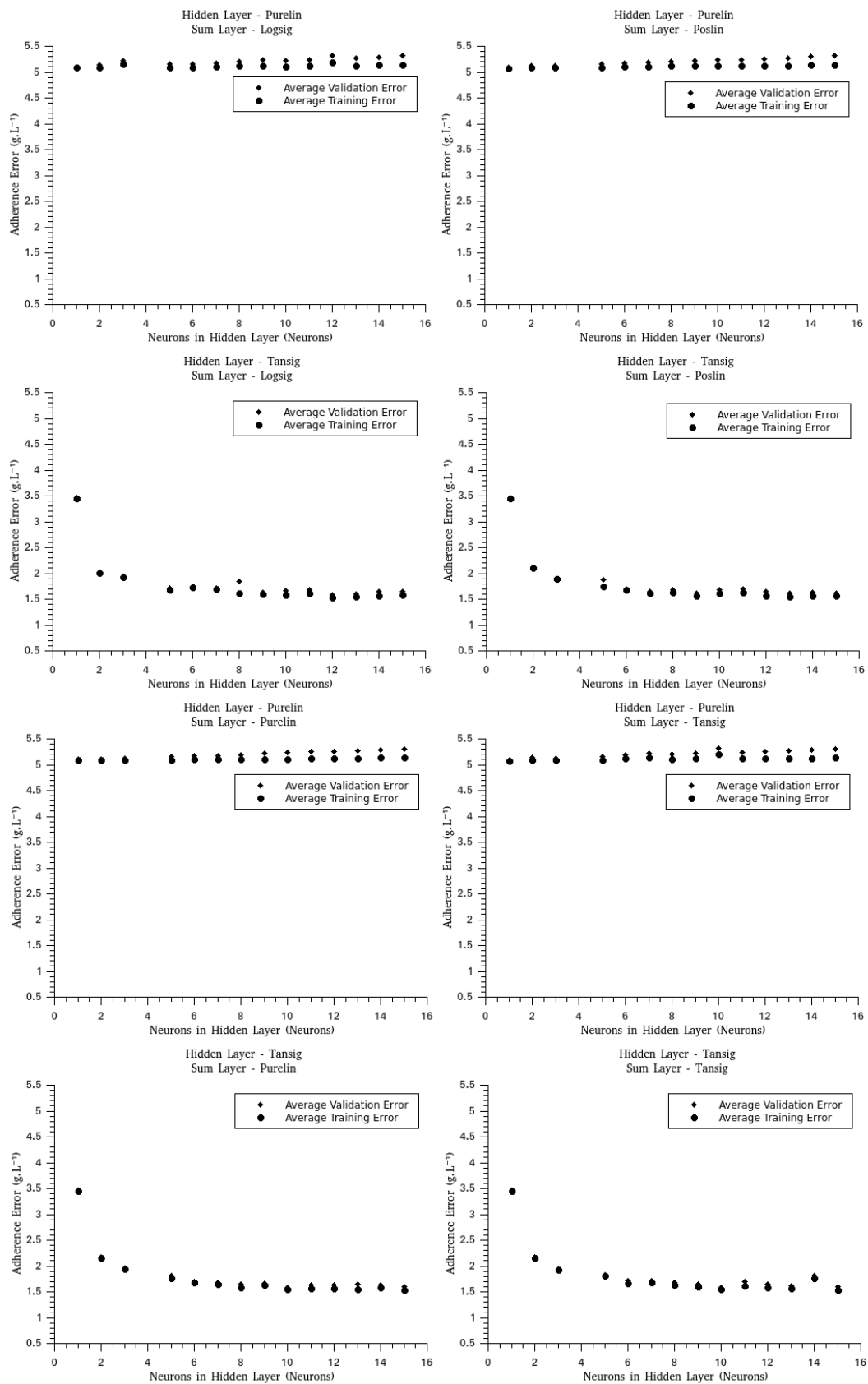
The values generated by the optimized model were used to train an artificial neural network to predict glucose concentration within the reactor. The input data were conductance, capacitance, agitation power, accumulated solids and reactor volume. The network errors for each network architecture are presented in Figure 28 and 29.

Figure 28 – Artificial Neural Network Errors – Poslin and Logsig Architectures



(Source: author's collection)

Figure 29 – Artificial Neural Network Errors – Poslin and Logsig Architectures

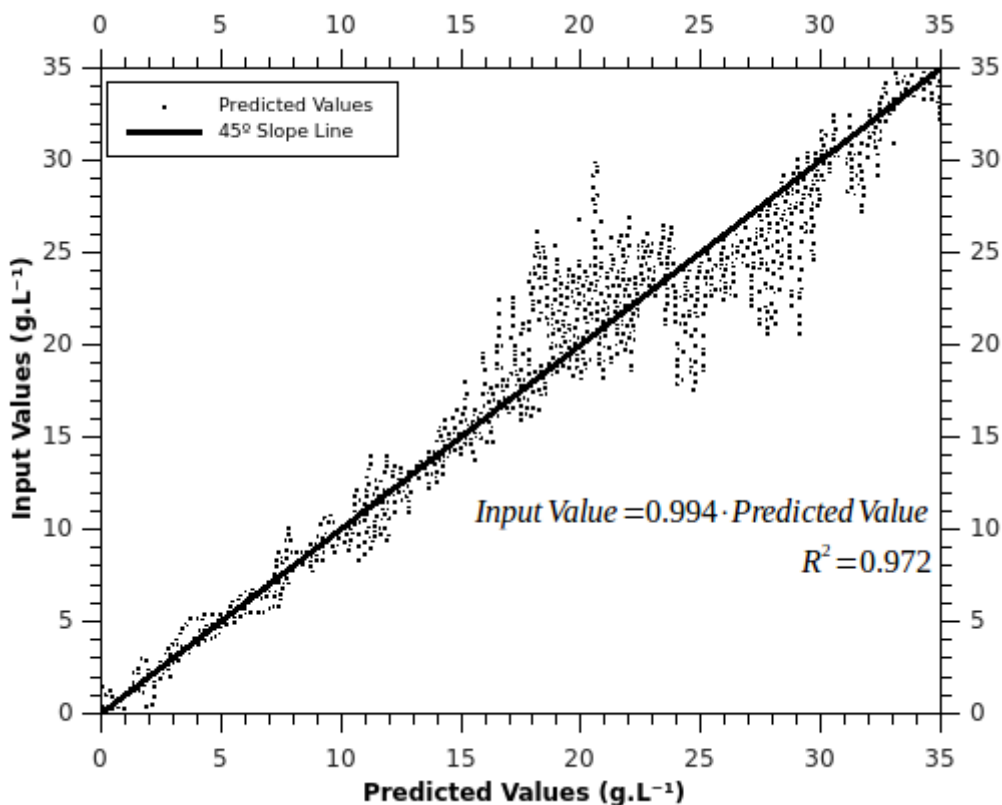


(Source: author's collection)

The majority of architectures presented, disregarding certain deviations, the behavior shown in Figure 9, except for the architectures containing a Pure Linear activation function in the hidden layer. The lowest average validation error occurred when the architecture contained a Tangent Sigmoid transfer function both in the hidden and sum layers, and with 11 neurons in the hidden layer. The addition of further neurons to this architecture generates an increase in the validation error, demonstrating that the optimum amount of neurons already occurred.

A scatter plot of the simulated glucose values and the ones predicted by the network is presented in Figure 30.

Figure 30 – Optimum Architecture Predicted Values



(Source: author's collection)

This figure demonstrates a linear relationship between the input values and the ones predicted by the ANN. The determination angular coefficient of the data is 0.994, demonstrating a strong correlation among the predicted and input values.

However, at high concentrations (larger than 12 g.L⁻¹) the dispersion becomes less stable. This may be explained by the fact that at these concentrations only batch data are available. This interferes in the prediction in two ways. First, less data are available in the

region, since the fed-batch experiments did not reached these concentrations of product. Second, these data are gathered at the final hours of the batch process, when the model used to generate the data becomes less adequate to describe the process, generating a deviation between the available data and the actual data.

However, the network demonstrated to be a promising tool in order to estimate the state of the reactor online, doing so regardless of the policy used in the reactor (batch or fed-batch). This network, or a variation of it, may be used in order to estimate the reaction kinetics in real time, and thus, generate feedback information to the controller software, enabling a closed-loop control strategy.

5. CONCLUSIONS

The first conclusion of this work is that the presented models were able to describe the hydrolysis to some extent. A departure between the experimental and predicted values arises in long term operations. This may be due to inhibition effects not described by the model. Thus, further inhibition studies need to be conducted so that the model may be more accurate.

The ANN, after architecture optimization, was capable of predicting product concentration from available data with a strong correlation (Determination Coefficient of 0.972). Therefore, the softsensor can be tested in further studies to generate feedback of data to the dynamic control software, in a closed loop architecture.

The optimization software was able to generate profiles that increased the process performance index while maintaining operational levels within the reactor, reaching glucose concentrations close to those utilized in current first generation technology even when a restriction to enzyme feed was applied (156.0 g.L^{-1} of glucose after 360h) or not (168.3 g.L^{-1}). However, using a stirred tank, fed-batch reactor in the industrial case would demand a, relatively, large plant (reactors ranging from 490 to 35,000 m^3). Thus, reactor design must improved in order to adequate this technology to industrial use.

6. FURTHER STUDIES SUGGESTIONS

Further study suggestions include:

- Performing experiments to evaluate enzymatic complex inhibition during the hydrolysis.
- Performing validation experiments with feeding strategies generated by the feeding optimizer.
- Generating a more complete model that correlates solids concentration with agitation power.
- Optimizing the ANN further, while using other tools in order to estimate reaction kinetics more accurately.
- Coupling a CTSR to the standard reactor to diminish the overall cost of the process.

REFERENCES

- ARANTES, V.; SADDLER, J. N. **Cellulose accessibility limits the effectiveness of minimum cellulase loading on the efficient hydrolysis of pretreated lignocellulosic substrates.** *Biotechnology Biofuels*, n. 4, p. 3, 2011.
- BANERJEE, S.; MUDALIAR, S.; SEN, R.; GIRI, B.; SATUPE, D.; CHAKRABARTI, T.; PANDEI, R. A. **Commercializing lignocellulosic bioethanol: technology bottlenecks and possible remedies.** *Biofuels Bioproducts & Biorefining-BioFPR*, v. 4, n. 1, p. 77 – 93, 2010.
- BANSAL, P.; HALL, M.; REALFF, M. J.; LEE, J. H.; BOMMARIUS, A. S. **Modeling cellulase kinetics on lignocellulosic substrates.** *Biotechnology Advances*, v. 27, p. 833 – 848, 2009.
- BANZI, M. **Getting started with Arduino.** Sebastopol, California, United States of America: O'Reilly Media Inc., 2009.
- BEZERRA, R. M. F.; DIAS, A. A. **Discrimination among eighth modified michaelis-mentem kinetics models of cellulose hydrolysis with large range substrate/enzyme ratios.** *Applied Biochemistry and Biotechnology*, v. 112, p. 173 – 181, 2004.
- BRYANT, D. N.; FIRTH E., KADERBHAI, N.; TAYLOR, S.; MORRIS, S. M.; LOGAN, D.; GARCIA, N.; ELLIS, A.; MARTIN, S. M.; GALLAGHER, J. A. **Monitoring real-time enzymatic hydrolysis of Distillers Dried Grains with Solubles (DDSG) by dielectric spectroscopy following hydrothermal pre-treatment by steam explosion.** *Bioresource Technology*, v. 128, p. 765 – 768, 2013.
- CARDONA, C. A.; QUINTERO, J. A.; PAZ, I. C. **Production of bioethanol from sugarcane bagasse: Status and perspectives.** *Bioresource Tecnology*, v. 101, p. 4754 – 4766, 2010.
- CANILHA, L.; CHANDEL, A. K.; MILESSI, T. S. S.; ANTUNES, F. A. F.; FREITAS, W. L. C.; FELIPE, M. G. A.; SILVA, S. S. **Bioconversion of sugarcane biomass into ethanol: an overview about composition, pretreatment methods, detoxification of hydrolysates, enzymatic saccharification, and ethanol fermentation.** *Journal of Biomedicine and Biotechnology*, v. 2012, 15 p., 2012.
- CARVALHO, M. L.; SOUZA JR., R.; RODRÍGUEZ-ZÚÑIGA, U. F.; SUAREZ, C. A. G., RODRIGUEZ, D. S.; GIORDANO, R. C.; GIORDANO, R. L. C. **Kinetic study of the**

- enzymatic hydrolysis of sugarcane bagasse.** Brazilian Journal of Chemical Engineering, v. 30, n. 3, p. 437 – 447, 2013.
- CAVALCANTI-MONTAÑO, I. D.; SUAREZ, C. A. G.; RODRÍGUEZ-ZÚÑIGA, U. F.; GIORDANO, R. L. C.; GIORDANO, R. C.; SOUZA, R. Jr. **Optimal bioreactor operational policies for the enzymatic hydrolysis of sugarcane bagasse.** Bioenergy Research, v. 6, p. 776 – 785, 2012.
- CHANDRA, R. P.; AU-YEUNG K.; CHANIS, C.; ROSS, A. A.; MABEE, W.; CHUNG, P. A.; GHATORA, S.; SADDLER, J. N. **The influence of pretreatment and enzyme loading on the effectiveness of batch and fed-batch hydrolysis of com stover.** Biotechnology Progress, v. 27, p 77 – 85, 2011 .
- CHIARAMONTI, D.; PRUSSI, M.; FERRERO, S.; ORIANI, L.; OTTONELLO, P.; TORRE, P.; CHERCHI, F. **Review of pretreatment processes for lignocellulosic ethanol production, and development of an innovative method.** Biomass and Bioenergy, n. 46, p. 23 – 35, 2012.
- DANTAS, G. A.; LEGEY, L. F. L.; MAZZONE, A. **Energy from sugarcane bagasse in Brazil: An assessment of the productivity and cost of different technological routes.** Renewable and Sustainable Energy Reviews, v. 21, p. 356 – 564, 2013.
- DEHURI, S.; CHO, S. B. **Multi-criterion pareto based particle swarm optimized polynomial neural network for classification: A review and state-of-art.** Computer Science Review, v. 3, p 19 – 40, 2009.
- DEMARTINI, J. D.; STUDER, M H.; WYMAN, C. E. **Small-scale and automatable high-throughput compositional analysis of biomass.** Biotechnology and Bioengineering, v. 108, n. 2, 2011.
- DIAS, M. O. S.; CUNHA, M. P.; JESUS, C. D. F.; ROCHA, G. J. M.; PRADELLA, J. G. C.; ROSSEL, C. E. V.; FILHO, R. M.; BONOMI, A. **Second generation ethanol in brazil: can it compete with electricity production?** Bioresource Technology, v. 102, p. 8964 – 8971, 2011.
- DIAS, M. O. S.; JUNQUEIRA, T. L.; CAVALLET, O.; CUNHA, M. P.; JESUS, C. D. F.; ROSSEL, C. E. V.; MACIEL FILHO, R.; BONOMI, A. **Integrated versus stand-alone second generation ethanol production from sugarcane bagasse and trash.** Bioresource Technology, v. 103, p. 152 – 161, 2012.
- EHRHARDT, M. R.; MONZ, T. O.; ROOT, T. W.; CONNELLY, R. K.; SCOTT, C. T.; KLINGENBERG, D. J. **Rheology of dilute acid hydrolyzed corn stover at high solids concentration.** Applied Biochemistry and Biotechnology, v. 160, p. 1102 –

1115, 2010.

FERNANDES, A. C. **Cálculos na agroindústria de cana-de-açúcar**. 2nd ed. Piracicaba: STAB, 2003. 240p.

FREITAS, L. C.; KANEKO, S. **Is there a casual relation between ethanol innovation and the market characteristics of fuels in brazil?** *Ecological Economics*, v. 74, p. 161 – 168, 2012.

FURLAN, F. F.; COSTA, C. B. B.; FONSECA, G. C.; SOARES, R. P.; SECCHI, A. R.; CRUZ, A. J. G., GIORDANO, R. C. **Assesing the production of first and second generation bioethanol from sugarcane through the integration of global optimization and process detailed modeling.** *Computers and chemical engineering*, v. 43, p. 1 – 9, 2012.

FURLAN, F. F.; TONON FILHO, R.; PINTO, F. H. P. B.; COSTA, C. B. B.; CRUZ, A. J. G.; GIORDANO, R. L. C.; GIORDANO, R. C. **Bioelectricity versus bioethanol from sugarcane bagasse: is it worth being flexible?** *Biotechnology for Biofuels*, v. 6, n. 1. p. 1 – 12, 2013.

GAMAGE, J.; HOWARD, L.; ZISHENG, Z **Bioethanol production from lignocellulosic biomass.** *Journal of Biobased Mater Bioenergy*, n. 4,p. 3 -11, 2010.

GOUVEIA, E. R.; NASCIMENTO, R. T.; ROCHA, G. J. M. **Validação da metodologia para a caracterização química de3 bagaço de cana-de-açúcar.** *Química Nova*, v. 32, p. 1500 – 1503, 2009.

GUPTA, R.; KUMAR, S.; GOMES, J.; KUHAD, R. C. **Kinetic study of batch and fed-batch enzymatic saccharification of pretreated substrate and subsequent fermentation to ethanol.** *Biotechnology for Biofuels*, v. 5, n. 16, p. 1 – 10, 2012.

HIMMELBLAU, D. M. **Process analysis by statistical methods.** New York, United States of America: John Wiley & Sons Inc, 1970.

HODGE, D. B.; KARIM, M. N.; SCHELL, D. J.; MCMILLAN, J. D. **Soluble and insoluble solids contribution to high-solids enzymatic hydrolysis of lignocellulose.** *Bioresource Technology*, v. 99, p 8940 – 8948, 2008.

HODGE, D. B.; KARIM, M. N.; SCHELL, D. J.; MCMILLAN, J. D. **Model-based fed-batch for high-solids enzymatic cellulose hydrolysis.** *Applied Biochemical Biotechnology*, v. 152, p. 88 – 107, 2009.

HORN, S. J.; VAAJE-KOLSTAD, G.; WESTERENG, B.; EIJSINK, V. G. H. **Novel enzymes for degradation of cellulose.** *Biotechnology for Biofuels*, v. 5, n. 45, 2012.

HUMBIRD, D.; MOHAGHEGHI, A.; DOWE, N.; SCHELL, D. J. **Economic impact of total**

- solids loading on enzymatic hydrolysis of dilute acid pretreated corn stover.** Biotechnology Progress, v. 26, n. 5, p. 1245 – 1251, 2010.
- JORGENSEN, H.; KRISTENSE, J. B.; FELBY, C. **Enzymatic conversion of lignocellulose into fermentable sugars: challenges and opportunities.** Biofuels Bioproducts and Biorefining, v. 1, n. 2, p. 119 – 134, 2007.
- KLINE, L. M.; HAYES, D. G.; WOMAC, A. R. **Simplified determination of lignin content in hard and soft woods via uv-spectrophotometric analysis of biomass dissolved in ionic liquids.** Bioresources, v. 5, n3., p. 1366 – 1383, 2010.
- KADLEC, P.; GABRYS, B.; STRANDT, S. **Data-driven soft sensors in the process industry.** Computers and Chemical Engineering, v. 33, p. 795 – 814, 2009.
- KIM, Y.; MOSIER, N. S.; LADISCH, M. R.; **Enzymatic digestion of liquid hot water pretreated hybrid poplar.** Biotechnology Progress, n. 8, p. 25 – 34, 2009.
- KRISTENSEN, J. B.; FELBY, C.; JORGENSEN, H. **Yield-determining Factors in High-solids Enzymatic Hydrolysis of Lignocellulose.** Biotechnology for Biofuels, v. 2, n. 11, p. 1 – 10, 2009.
- KUPSKI, L.; PAGNUSSATT, F. A.; GUARDA-BUFFON, J.; BADIALE-FURLONG, E. **Endoglucanase and total cellulase from newly isolated *Rhizopus oryzae* and *Trichoderma reesei*: Production, Characterization, and Thermal Stability.** Applied Biochemistry and Biotechnology, DOI 10.1007/s12010-013-0518-2, 2013.
- LIMAYEM A., RICKE, S. C. **Lignocellulosic biomass for bioethanol production: Current perspectives, potential issues and future prospects.** Progress in Energy and Combustion Science 38, v. 38, p. 449 – 467, 2012.
- KARIMI, J., NOBAHARI, H., POURTAKDOUST, S. H. **A new hybrid approach for dynamic continuous optimization problems.** Applied Soft Computing, v. 12, p. 1158 – 1167, 2012.
- MACRELLI, S.; MOGENSEN, J.; ZACCHI, G. **Techno-economic evaluation of 2nd generation bioethanol production from sugar cane bagasse and leaves integrated with the sugar-based ethanol process.** Biotechnology for Biofuels, p. 5:22, 2012.
- MENON, V.; RAO, M. **Trends in bioconversion of lignocellulose: biofuels, platform chemical & biorefinery concept.** Progress in Energy and Combustion Science, v. 38, p. 522 – 550, 2012.
- MODENBACH, A. A.; NOKES, S. E. **Enzymatic hydrolysis of biomass at high-solids loadings – A review.** Biomass and Bioenergy, v. 56, p 526 – 544, 2013.

- MICHAELIS, L.; MENTEN, M.L. **Die kinetik der invertinwirkung.** Biochemische Zeitschrift, v. 49, n. 3, p. 333 – 369, 1913.
- MORALES-RODRÍGUEZ, R.; CAPRON, M.; HUUSOM, J. K.; SIN, G. **Controlled fed-batch operation for improving cellulose hydrolysis in 2g bioethanol production.** In: 20th European Symposium on Computer Aided Process Engineering – ESCAPE20
- NAGY, Z. K.; BRAATZ, R. D. **Open-loop and closed-loop optimal control of batch processes using distributional and worst-case analysis.** Journal of Process Control, v. 14, p 411 – 422, 2004.
- NAIK, S. N.; GOUD, V. V.; ROUT, P. K.; DALAI, A. K. **Production of first and second generation biofuels: A comprehensive review.** Renewable and Sustainable Energy Reviews, v. 14, p. 578 – 597, 2010.
- NELLES, O. **Nonlinear system identification: From classical approaches to neural networks and fuzzy models.** Berlin Heidelberg, Germany: Springer-Verlag, 2001.
- NREL. **Determination of structural carbohydrates and lignin in biomass.** Biomass Program Analysis Technology Team Laboratory Procedure, National Renewable Energy Lab (NREL/TP-510-42618).
- RAMIREZ, W. F. **Process control and identification.** São Diego, California, Estados Unidos da América: Academic Press Inc., 1994.
- RIBEIRO, M. P. A.; GIORDANO, R. C. **Variational calculus (optimal control) applied to the optimization of the enzymatic synthesis of ampicillin.** Brazilian Archives of Biotechnology and Technology, v. 48, p. 19 – 28, 2005.
- ROCHA, G. J. M.; MARTIN, C.; SOARES, I. B. **Diluted mixed-acid pretreatment of sugarcane bagasse for ethanol production.** Biomass and energy, v. 35, n. 1, p. 663 – 670, 2011.
- RODRIGUEZ-ZÚÑIGA, U. F.; FARINAS, C. S.; CARNEIRO, R. L.; SILVA, G. M.; CRUZ, A. J. G.; GIORDANO, R. L. C.; GIORDANO, R. C. G.; RIBEIRO, M. P. A. **Fast determination of the composition of pretreated sugarcane bagasse using near-infrared spectroscopy.** Bioenergy Resource, v. 7, p. 1441 – 1453, 2014.
- SANTOS, F. A.; QUEIRÓZ, J. H.; COLODETTE, J. L.; FERNANDES, S. A.; SEBASTIÃO, V. M. G.; REZENDE, T. **Potential de palha de cana-de-açúcar para produção de etanol.** Química Nova, v. 35, n. 5, p. 1004 – 1010, 2012.

- SAMANIUK, J. R.; SCOTT, C. T.; ROOT, T. W.; KLINGENBERG, D. J. **The effect of high intensity mixing on the enzymatic hydrolysis of concentrated cellulose fiber suspension.** *Bioresource Technology*, v. 102, p. 4489 – 4494, 2011.
- SLUITER, J. B.; RUIZ, R. O.; SCARLATA, C. J.; SLUITER A. D.; TEMPLETON, D. W. **Compositional analysis of lignocellulosic feedstocks. 1. Review and description of methods.** *Journal of Agricultural and Food Chemistry*, n. 58, p. 9043 – 9053, 2010.
- SOUSA JR, R.; CARVALHO, M. L.; GIORDANO, R. L. C.; GIORDANO, R. C. **Recent trends in the modeling of cellulose hydrolysis.** *Brazilian Journal of Chemical Engineering*, v. 28, n. 4, p. 545 – 564, 2011.
- SRINIVASAN, B.; PALANKI, S.; BOVIN, D. **Dynamic optimization of batch processes i. characterization of nominal solution.** v. 27, p. 1 – 27, 2003.
- STEWART, D. **Lignin as a base material for materials applications: Chemistry, application and economics.** *Industrial Crops and Products*, v. 27, n. 2, p. 202 – 207, 2008.
- SUN, Y.; CHENG, J. **Hydrolysis of lignocellulosic materials for ethanol production: A review.** *Boiresource Technology*, v. 83, p. 1 -11, 2002.
- THONGEKKAEW, J.; IKEDA, H.; MASAKI, K.; IEFUJI, H. **an acidic and thermostable carboxymethyl cellulase from *cryoticiccus* sp. s-2: purification, characterization and improvement of its recombinant enzyme production by high cell density fermentation of *pichia pastori*.** *Protein Expression and Purification*, v. 60, p. 144 – 146, 2008.
- TOMÁS, R. L.; OLIVEIRA, J. C.; MCCARTHY, K. L. **Influence of operating conditions on the extent of enzymatic conversion of rice starch in wet extrusion.** *LWT – Food Science and Technology*, v. 30, p. 50 – 55, 1997.
- UPETRI, S. R. **Optimal control for chemical engineers.** Boca Raton, Florida, Estados Unidos da América: CRC Press, 2013.
- VOJINOVIC, V.; CABRAL, J. M. S.; FONSECA, L. P. **Real-time bioprocess monitoring Part I: In situ sensors.** *Sensors and Actuators*, v. 114, p. 1083 – 1091, 2006.
- WANG, L.; TEMPLER, R.; MURPHY, R. J. **High-solids loading enzymatic hydrolysis of waste papers for biofuel production.** *Applied Energy*, v. 99, p. 23 – 31, 2012.
- WYMAN, C. E. **Potential synergies and challenges in refining cellulosic biomass to**

fuels, chemicals and power. Biotechnology Progress, v. 19, p. 254 – 262, 2003.

XU, F.; YU, J.; TESSO, T.; DOWELL, F.; WANG, D. **Qualitative and quantitative analysis of lignocellulosic using infrared techniques: A mini-review.** Applied Energy, n. 104, p. 801 – 809, 2013.

ZHANG, Y. P.; LYND, L. R. **Toward an aggregated understanding of enzymatic hydrolysis of cellulose: Noncomplexed cellulase systems.** Biotechnology and Bioengineering, v. 88, n.7, 2004.